

**Discovery of 4-Phenylpiperidine-2-Carboxamide Analogues as Serotonin 5-HT<sub>2C</sub> Receptor Positive Allosteric Modulators with Enhanced Drug-Like Properties**

Eric A. Wold, Erik J. Garcia, Christopher Wild, Joanna M. Miszkiet, Claudia A Soto, Jianping Chen, Konrad Pazdrak, Robert G Fox, Noelle C. Anastasio, Kathryn A. Cunningham, and Jia Zhou

*J. Med. Chem.*, **Just Accepted Manuscript** • DOI: 10.1021/acs.jmedchem.9b01953 • Publication Date (Web): 22 Jun 2020

Downloaded from pubs.acs.org on June 22, 2020

**Just Accepted**

"Just Accepted" manuscripts have been peer-reviewed and accepted for publication. They are posted online prior to technical editing, formatting for publication and author proofing. The American Chemical Society provides "Just Accepted" as a service to the research community to expedite the dissemination of scientific material as soon as possible after acceptance. "Just Accepted" manuscripts appear in full in PDF format accompanied by an HTML abstract. "Just Accepted" manuscripts have been fully peer reviewed, but should not be considered the official version of record. They are citable by the Digital Object Identifier (DOI®). "Just Accepted" is an optional service offered to authors. Therefore, the "Just Accepted" Web site may not include all articles that will be published in the journal. After a manuscript is technically edited and formatted, it will be removed from the "Just Accepted" Web site and published as an ASAP article. Note that technical editing may introduce minor changes to the manuscript text and/or graphics which could affect content, and all legal disclaimers and ethical guidelines that apply to the journal pertain. ACS cannot be held responsible for errors or consequences arising from the use of information contained in these "Just Accepted" manuscripts.

Discovery of 4-Phenylpiperidine-2-Carboxamide Analogues as  
Serotonin 5-HT<sub>2C</sub> Receptor Positive Allosteric Modulators with  
Enhanced Drug-Like Properties

Eric A. Wold,<sup>†,‡,¶</sup> Erik J. Garcia,<sup>†,¶</sup> Christopher T. Wild,<sup>†,‡,¶</sup> Joanna M. Miszkiel,<sup>†</sup> Claudia A.  
Soto,<sup>†</sup> Jianping Chen,<sup>†,‡</sup> Konrad Pazdrak,<sup>†</sup> Robert G. Fox,<sup>†</sup> Noelle C. Anastasio,<sup>†,‡,\*</sup> Kathryn A.  
Cunningham,<sup>†,‡,\*</sup> and Jia Zhou<sup>†,‡,\*</sup>

<sup>†</sup>Center for Addiction Research and <sup>‡</sup>Chemical Biology Program, and the Department of  
Pharmacology and Toxicology, University of Texas Medical Branch, Galveston, TX 77555,  
United States

<sup>¶</sup>Authors contributed equally to this work

\*Corresponding authors

## Abstract

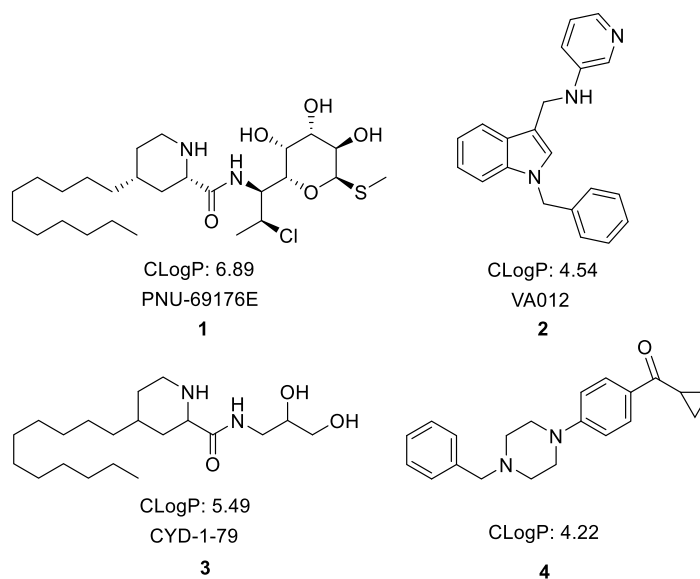
Targeting the serotonin (5-HT) 5-HT<sub>2C</sub> receptor (5-HT<sub>2C</sub>R) allosteric site to potentiate endogenous 5-HT tone may provide novel therapeutics to alleviate the impact of costly, chronic diseases such as obesity and substance use disorders. Expanding upon our recently described 5-HT<sub>2C</sub>R positive allosteric modulators (PAMs) based on the 4-alkylpiperidine-2-carboxamide scaffold, we optimized the undecyl moiety at the 4-position with variations of cyclohexyl- or phenyl-containing fragments to reduce rotatable bonds and lipophilicity. Compound **12** (CTW0415) was discovered as a 5-HT<sub>2C</sub>R PAM with improved pharmacokinetics and reduced off-target interactions relative to our previous series of molecules. The *in vivo* efficacy of compound **12** to potentiate the effects of a selective 5-HT<sub>2C</sub>R agonist was established in a drug discrimination assay. Thus, **12** is reported as a 5-HT<sub>2C</sub>R PAM with characteristics suitable for *in vivo* pharmacological studies to further probe the biological and behavioral mechanisms of allosteric modulation of a receptor important in several chronic diseases.

## Introduction

Neuropsychiatric and metabolic disorders currently encompass exceedingly costly and intractable diseases both in the U.S. and worldwide. Indeed, obesity and substance use disorders (SUDs) can manifest as chronic conditions that dramatically reduce life expectancy. The serotonin (5-HT) 5-HT<sub>2C</sub> receptor (5-HT<sub>2C</sub>R) is a predominately central nervous system (CNS) G protein-coupled receptor (GPCR) that modulates key disease-related neurological pathways and behaviors.<sup>1</sup> For example, 5-HT<sub>2C</sub>R agonists suppress food intake and increase satiety in humans and animals,<sup>2-6</sup> and preclinical studies indicate a major role for the 5-HT<sub>2C</sub>R in modulating the rewarding and incentive-salience value of psychostimulants (e.g., cocaine), opioids, and ethanol as well as behavioral factors predictive of relapse during SUD recovery.<sup>7-11</sup> In human studies, the 5-HT<sub>2C</sub>R agonist lorcaserin increased the rate of cessation from tobacco smoking, and decreased corticolimbic activation evoked by presentation of palatable food cues, thus implicating the 5-HT<sub>2C</sub>R as a target mechanism for disorders characterized by reward and cue-associated events.<sup>12</sup> Therefore, the 5-HT<sub>2C</sub>R is a favorable therapeutic target at the intersection of disinhibited behaviors that promote obesity and SUDs, and a pharmacotherapy that could aid in the successful treatment of SUDs would be a first-in-class medication.<sup>14, 15</sup>

Selective targeting of the 5-HT<sub>2C</sub>R remains challenging since each of the 13 5-HT GPCR subtypes share a conserved orthosteric binding site for the endogenous agonist 5-HT. Among the 5-HT<sub>2</sub>R subtypes (5-HT<sub>2A</sub>R, 5-HT<sub>2B</sub>R, and 5-HT<sub>2C</sub>R), 5-HT<sub>2C</sub>R selectivity is necessary to avoid the potential for hallucinations or cardiac valvulopathy that may result as a consequence of 5-HT<sub>2A</sub>R or 5-HT<sub>2B</sub>R stimulation, respectively.<sup>16, 17</sup> One possible strategy to achieve selective 5-HT<sub>2C</sub>R modulation is the rational design of positive allosteric modulators (PAMs).<sup>18</sup> By targeting

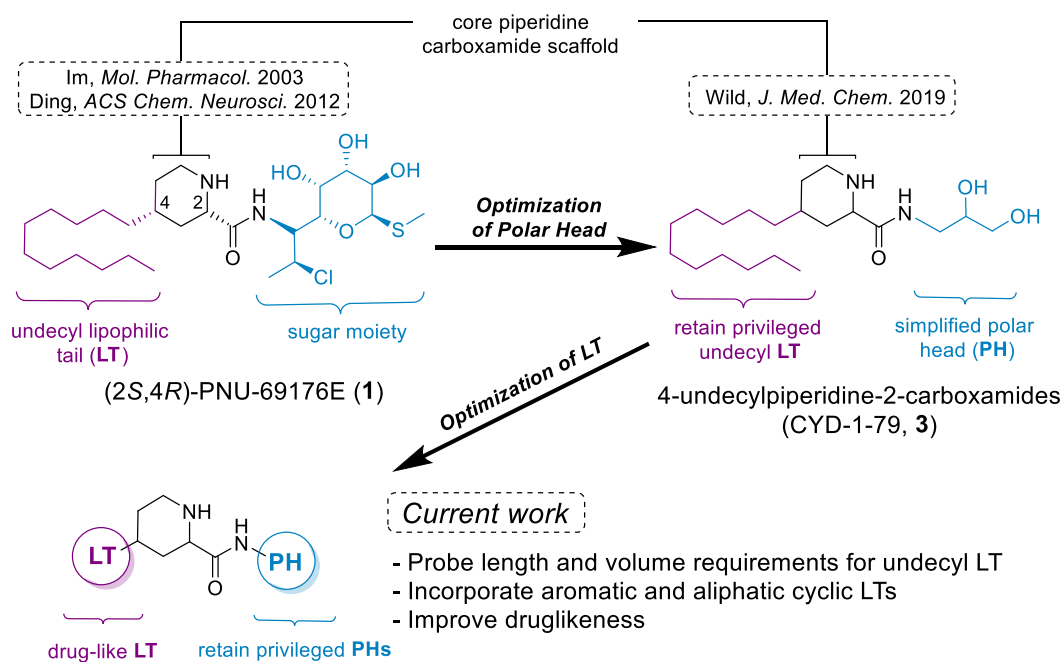
a binding site that is spatially distinct from the conserved 5-HT orthosteric site, divergent residues or topological surfaces may be exploited to achieve 5-HT<sub>2C</sub>R selectivity while enhancing the functional response to 5-HT.<sup>19</sup> This strategy has been employed for numerous class A GPCRs<sup>20</sup> and specifically for the discovery of 5-HT<sub>2C</sub>R PAMs by our group and others (**Figure 1**).<sup>21-25</sup>



**Figure 1. Highlighted compounds resulting from the search for synthetic small molecule 5-HT<sub>2C</sub>R PAMs.** Highlighted here are lead compounds from the published 5-HT<sub>2C</sub>R PAM drug discovery campaigns. The ClogP, calculated in ChemDraw 18.0, for each compound displays a trend in high lipophilicity.

Our previously described 5-HT<sub>2C</sub>R PAMs were obtained by an iterative exploration and optimization process beginning with the initial 5-HT<sub>2C</sub>R PAM small molecule PNU-69176E (**1**). The first priority in this process was the simplification of the  $\alpha$ -D-galactopyranoside fragment, termed the polar head (PH), to provide a more drug-like compound for *in vitro* and *in vivo* proof of concept studies (**Figure 2**). From this effort, CYD-1-79 (**3**) was obtained and characterized as a selective 5-HT<sub>2C</sub>R PAM (**Figure 1**).<sup>23</sup> The PH moiety of **3** was modified to retain 5-HT<sub>2C</sub>R PAM activity while engendering decreased molecular weight and complexity. Next, modifications to the

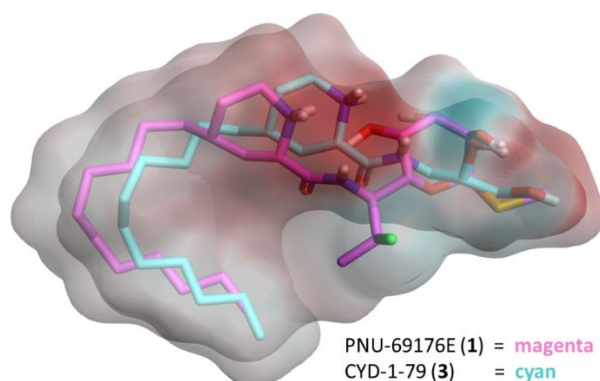
undecyl substituent at the 4-position of the piperidine, which is termed the lipophilic tail (LT), were probed as an option for further improvements. In the current study, we chemically modified the LT position with shorter, compact fragments to reduce lipophilicity while maintaining 5-HT<sub>2C</sub>R PAM activity (**Figure 2**). Additionally, we rationalized that the compact LT substituents would reduce the number of rotatable bonds and improve the drug-likeness of the 4-alkylpiperidine-2-carboxamide scaffold, which was further demonstrated by the calculated physicochemical properties for the synthesized test compounds herein (**Table S1**). Importantly, modifying the undecyl LT position with compact, cyclic moieties – providing increased structural rigidity – yielded small molecules that are advantageous for computational molecular modeling and docking studies to ultimately illuminate features of the 5-HT<sub>2C</sub>R PAM binding site.



**Figure 2. Medicinal chemistry strategy to achieve optimized 5-HT<sub>2C</sub>R PAMs from PNU-69176E (1).** A lincomycin derivative, PNU-69176E (1), was the first synthetic small molecule reported to allosterically modulate the 5-HT<sub>2C</sub>R. Subsequent work has focused on chemical modifications of the polar head (PH) and the lipophilic tail (LT) to engender drug-like properties.

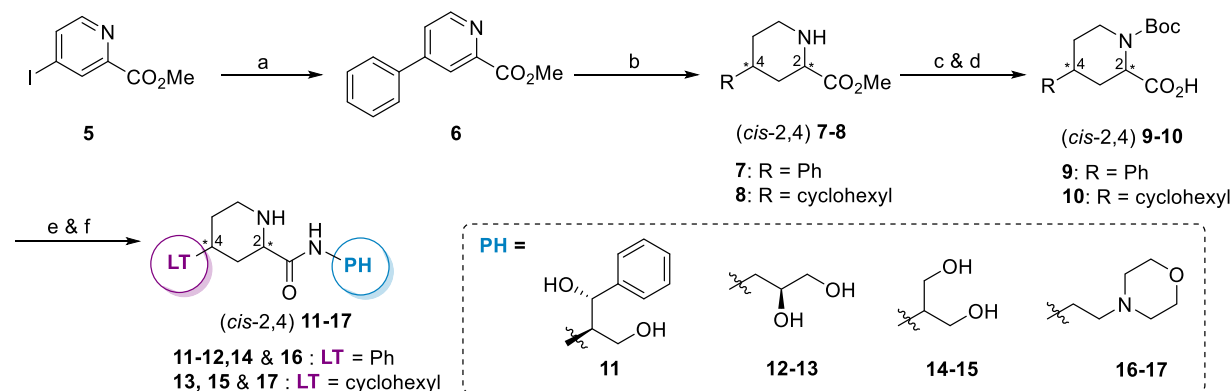
## Results and Discussion

**Chemistry.** Allosteric modulation of the 5-HT<sub>2C</sub>R is a new endeavor with a small number of probe compounds identified in recent years.<sup>23-25</sup> Our chemical approach is focused on the optimization of our previously reported compound **3**. Elevation of intracellular calcium (Ca<sub>i</sub><sup>2+</sup>) release is a key downstream impact of 5-HT<sub>2C</sub>R activation which is oft utilized as a readout in functional cellular assays.<sup>26</sup> Compound **3** was shown to enhance Ca<sub>i</sub><sup>2+</sup> release ~23% above the maximal effect of 5-HT alone in Chinese hamster ovary (CHO) cells stably transfected with human (h)5-HT<sub>2C</sub>R. In the absence of 5-HT, **3** had no effect on Ca<sub>i</sub><sup>2+</sup> release, indicating the PAM nature of this compound. Compound **3** also exhibited *in vivo* efficacy to decrease locomotor activity and suppress cocaine-seeking during abstinence from cocaine self-administration in rats; **3** potentiated the substitution of low doses of the 5-HT<sub>2C</sub>R agonist WAY163909 in a drug discrimination assay.<sup>23</sup> Therefore, the 1,2-diol moiety in the PH position of **3** was considered a privileged fragment and was retained. Additional PH fragments were employed in the following chemical series based upon their previously observed activity or inactivity as a basis of comparison.



**Figure 3. The volume, not length, of the undecyl moiety on PNU-69176E (1) and CYD-1-79 (3) may contribute to 5-HT<sub>2C</sub>R PAM activity.** Compounds **1** and **3** favor similar minimized conformations which leads to overlapping hydroxyl moieties in the PH and to a folded substructure for the undecyl LT. The preferred, contracted substructure for the undecyl LT suggests that hydrophobic volume is important.

Initial structure-activity relationship (SAR) studies of compound **1** showed that shorter alkyl chains (methyl to *n*-methyl groups) as LTs failed to exert positive allosteric modulatory actions at the 5-HT<sub>2</sub>cR;<sup>21</sup> however we reasoned that the volume of the LT, not the length, may play a role in compound activity. This hypothesis was based partially upon *in silico* ligand minimization and electrostatic complementarity experiments comparing compound **1** with compound **3** (**Figure 3**). First, the modeling shows how the replacement of the  $\alpha$ -D-galactopyranoside PH fragment with the simplified 1,2-diol fragment found in **3** retains key hydroxyl group orientations and thus potentially conserve H-bond partners and interaction distances. Second, the minimized alignment of the undecyl LT fragments are shown in a conformation that suggests an exploitation of a hydrophobic binding pocket due to lipophilic volume. Thus, we designed new small molecules to incorporate shorter LTs with aromatic and aliphatic rings able to provide a comparable volume to the longer alkyl chain counterparts. Crucially, these new analogues reduce the overall number of rotatable bonds and engender enhanced drug-like properties and development potential.

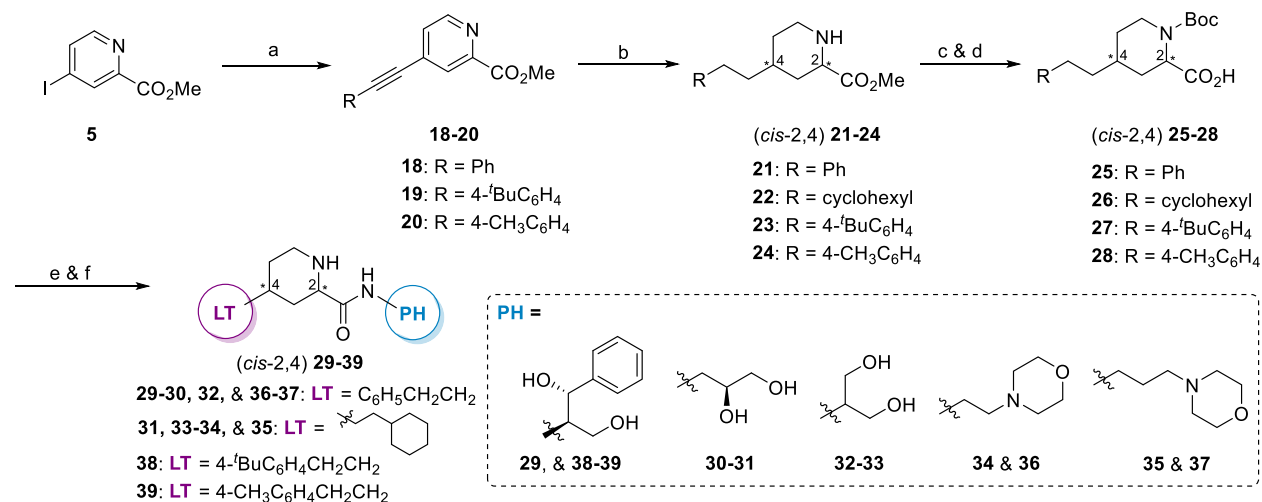


### Scheme 1. Synthesis of CYD-1-79 analogues with compact phenyl or cyclohexyl LTs

Reagents and conditions: a) phenylboronic acid, Pd(PPh<sub>3</sub>)<sub>4</sub>, Na<sub>2</sub>CO<sub>3</sub>, EtOH/H<sub>2</sub>O/PhMe = 2:1:1, reflux. b) H<sub>2</sub>, PtO<sub>2</sub>, HCl/MeOH/H<sub>2</sub>O, rt, 16 h. c) (Boc)<sub>2</sub>O, Et<sub>3</sub>N, MeOH, rt, 16 h. d) LiOH, THF/H<sub>2</sub>O (v/v = 2:1), rt, 48 h. e) amino alcohols, HBTU, DIPEA, DMF, rt, 16 h. f) TFA, CH<sub>2</sub>Cl<sub>2</sub>, rt.



Similar to our previously established synthetic route, a six-step protocol from **5** affords the target compounds.<sup>22, 23</sup> The iodinated ester of picolinic acid (**5**) underwent Suzuki (**Scheme 1**) or Sonogashira coupling (**Scheme 2**) to provide incorporation of various LTs that included aromatic rings (e.g., phenyl, phenethyl, 4'-methylphenethyl, and 4'-*t*-butylphenethyl fragments). Metal-catalyzed hydrogenation, Boc-protection, and hydrolysis readily provided the (*cis*-2,4)-piperidyl carboxylic acids **9-10** and **25-28**. As a result of the metal-catalyzed reduction conditions, the pyridine ring was consistently reduced, whereas the aromatic LTs either did not undergo hydrogenation or were fully reduced into separable products. Therefore, isolable aliphatic versions of the aromatic LTs were obtained, and upon HBTU-mediated coupling to suitable amines and N-Boc deprotection, target compounds **11-17** and **29-39** were obtained. All isomers with the 2-amino-1-phenyl-1,3-propanediol PH were separable, consistent with our previous report.<sup>23</sup> All other compounds were an inseparable mixture of isomers and were tested as such (**Schemes 1 & 2**).



## Scheme 2. Synthesis of CYD-1-79 analogues with phenethyl, ethylcyclohexyl, or substituted phenethyl LTs

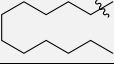
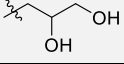
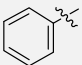
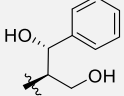
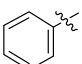
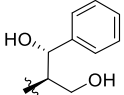
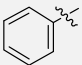
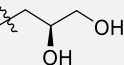
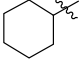
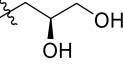
Reagents and conditions: a) Phenylacetylenes, CuI, Pd(PPh<sub>3</sub>)<sub>2</sub>Cl<sub>2</sub>, Et<sub>3</sub>N, rt, 12 h. b) H<sub>2</sub>, PtO<sub>2</sub>, HCl/MeOH/H<sub>2</sub>O, rt, 16 h. c) (Boc)<sub>2</sub>O, Et<sub>3</sub>N, MeOH, rt, 16 h. d) LiOH, THF/H<sub>2</sub>O (v/v = 2:1), rt, 48 h. e) amino alcohols, HBTU, DIPEA, DMF, rt, 16 h. f) TFA, CH<sub>2</sub>Cl<sub>2</sub>, rt.

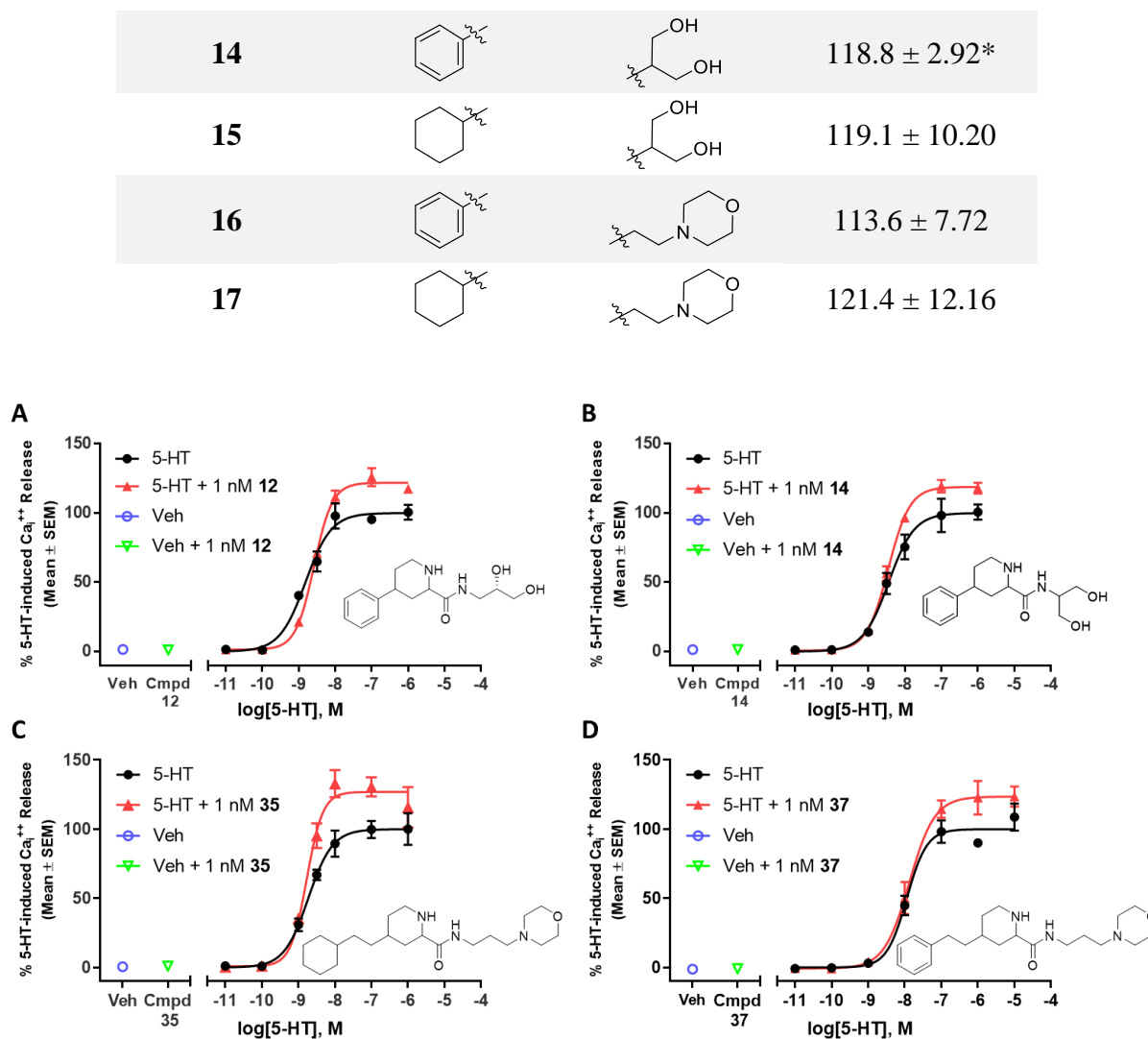
**Compound Screening *In Vitro*.** A very well characterized intracellular signaling pathway of the 5-HT<sub>2C</sub>R is the stimulation of phospholipase C $\beta$  via G $\alpha_{q/11}$  proteins leading to the production of inositol-1,4,5-trisphosphate and diacylglycerol, resulting in Ca<sub>i</sub><sup>2+</sup> release from intracellular stores.<sup>27</sup> Thus, a fluorescence-based, *in vitro* Ca<sub>i</sub><sup>2+</sup> release assay was utilized to measure activation of this 5-HT<sub>2C</sub>R signaling pathway and provide functional characterization of the newly synthesized compounds. Chinese hamster ovary (CHO) cells stably transfected with the human 5-HT<sub>2C</sub>R (unedited INI isoform; h5-HT<sub>2C</sub>R-CHO cells) were used for screening of compounds in the Ca<sub>i</sub><sup>2+</sup> release assay. The maximum 5-HT-induced Ca<sub>i</sub><sup>2+</sup> release ( $E_{\max}$ ) was measured and normalized to 100% response. All test compounds were assessed in 4-6 biological replicates, each conducted in technical triplicates and results are shown relative to the  $E_{\max}$  of 5-HT alone. Compound **1** increased 5-HT-evoked release in titration studies and evoked a leftward shift of the 5-HT-evoked Ca<sub>i</sub><sup>2+</sup> response curve.<sup>22</sup> Therefore, the initial compound screen was conducted at 1 nM to determine the extent to which compounds enhanced Ca<sub>i</sub><sup>2+</sup> release elicited by increasing concentrations of 5-HT. Each test compound was added to the h5-HT<sub>2C</sub>R-CHO cells 15 min prior to the addition of 5-HT to determine intrinsic agonist activity. None of the compounds tested exhibited intrinsic activity to induce Ca<sub>i</sub><sup>2+</sup> release in h5-HT<sub>2C</sub>R-CHO prior to the addition of 5-HT (**Figure S1**). The assessment of compounds tested in the Ca<sub>i</sub><sup>2+</sup> release assay in h5-HT<sub>2C</sub>R-CHO cells is shown in **Table 1** and **Table 2**, and all concentration response curve shift plots are in **Figure S1**.

Of the 22 compounds tested, several displayed 5-HT<sub>2C</sub>R PAM activity comparable to the previously reported **3** which displayed an approximate 23% increase in the  $E_{\max}$  for 5-HT-induced Ca<sub>i</sub><sup>2+</sup> release in h5-HT<sub>2C</sub>R-CHO cells.<sup>23</sup> Compounds **(2S,4R)-11** and **(2R,4S)-11** included a phenyl ring as the LT and incorporated a (1S,2S)-2-amino-1-phenyl-1,3-propanediol PH (**Table 1**). In our

previous report, when combined with an undecyl LT, the (1*S*,2*S*)-2-amino-1-phenyl-1,3-propanediol PH displayed negative allosteric modulatory (NAM) activity in (2*S*,4*R*) conformation.<sup>23</sup> However, (2*S*,4*R*)-**11** showed no activity while (2*R*,4*S*)-**11** displayed modest allosteric activity in the  $\text{Ca}^{2+}$  assay. Intriguingly, both **12** and **13**, which incorporate an isomer [(*S*)-1,2-diol] of the same 1,2-diol moiety PH as compound **3**, displayed 5-HT-evoked  $E_{\text{max}}$  values of  $127.4 \pm 8.79\%$  ( $p < 0.05$ ; **Figure 4A**) and  $117.9 \pm 4.71\%$  ( $p < 0.05$ ), respectively, close to the activity seen for **3** ( $123.2 \pm 4.1\%$ ,  $p < 0.05$ ).<sup>23</sup> This outcome was observed even though the new analogues possess a phenyl ring and a cyclohexyl ring as the LT (**12** and **13**, respectively), which is an extreme departure from the eleven-carbon tail in our previously reported compounds. These findings provide additional confirmation that the 1,2-diol moiety is a privileged fragment. The 1,3-propandiol as a PH did promote PAM activity when coupled with a phenyl LT (**14**,  $118.8 \pm 2.92\%$ ,  $p < 0.05$ ; **Figure 4B**). The same PH with a cyclohexyl LT (**15**) and the retention of the phenyl or cyclohexyl LT with incorporation of a morpholino with a two-carbon spacer (**16** and **17**, respectively) did not result in positive allosteric effects.

**Table 1. Effects of 4-alkylpiperidine-2-carboxamide derivatives (1 nM) on 5-HT-induced  $\text{Ca}^{2+}$  release in h5-HT<sub>2C</sub>R-CHO cells**

Compound Number	LT	PH	$E_{\text{max}}$ RFU (% 5-HT) <sup>a</sup>
<b>3</b>			$123.2 \pm 4.1^*$
(2 <i>S</i> ,4 <i>R</i> )- <b>11</b>			$102.9 \pm 7.67$
(2 <i>R</i> ,4 <i>S</i> )- <b>11</b>			$118.2 \pm 2.39^*$
<b>12</b>			$127.4 \pm 8.79^*$
<b>13</b>			$117.9 \pm 4.71^*$

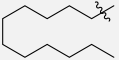
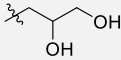
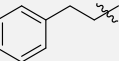
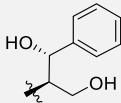
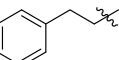
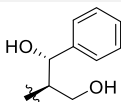
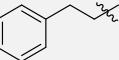

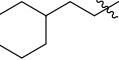
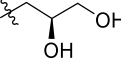
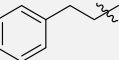
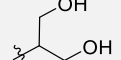
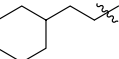
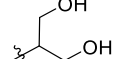
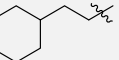
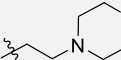


**Figure 4.** Effects of select compounds with shortened lipophilic tail (LT) moieties provide evidence that hydrophobic volume contributes to target engagement. Data are plotted for compounds **12** (A), **14** (B), **35** (C), and **37** (D). The effects of these compounds on 5-HT-induced  $\text{Ca}_i^{2+}$  release in h5-HT<sub>2C</sub>R-CHO cells are shown in the absence (black) and presence of the test compound (red) against the concentration-response curve for 5-HT. The assessment of vehicle (HBSS, blue circle), or vehicle with test compound (green triangle) is also illustrated.

Utilization of the PHs while incorporating either phenethyl or ethylcyclohexyl LTs resulted in a series of molecules with a range of activity (~94% - ~117%) dependent upon the type of PH incorporated (**Table 2**). Positive allosteric effects were not seen with the 1,2-diol and 1,3-diol PHs with either aforementioned LT (compounds **30** – **33**). For both the ethylcyclohexyl and phenethyl

LT, the two-carbon spaced morpholino as the PH did not produce PAM effects (**34**, **36**). However, the addition of the morpholino with a three-carbon spacer did produce PAM effects, suggesting there is a length requirement for morpholino fragment compounds (**35**,  $118.2 \pm 3.61\%$ ,  $p < 0.05$ ; **Figure 4C**; **37**,  $117.9 \pm 5.90\%$ ,  $p < 0.05$ ; **Figure 4D**). An increase in the length and volume of the LT via the inclusion of a *t*-butyl or methyl in the 4-position of the phenethyl LT did not lead to active compounds (**38** – **39**), an interesting finding given previous suggestions that LT length is a critical component of PAM activity for this chemotype.<sup>21</sup> These data reinforce the notion that a diol moiety PH, specifically an (*S*)-1,2-diol fragment, is an important structural element in 5-HT<sub>2C</sub>R PAMs (compounds **3** and **12**) and that the 5-HT<sub>2C</sub>R PAM pharmacophore is accepting of compact, cyclic LTs.

**Table 2. Effects of 4-alkylpiperidine-2-carboxamide derivatives (1 nM) on 5-HT-induced Ca<sub>i</sub><sup>2+</sup> release in h5-HT<sub>2C</sub>R-CHO cells**

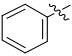
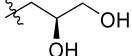
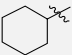
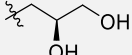
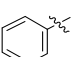
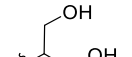
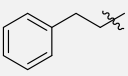
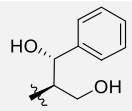
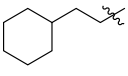
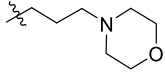
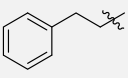
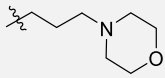
Compound Number	LT	PH	E <sub>max</sub> RFU (%5-HT) <sup>a</sup>
<b>3</b>			$123.2 \pm 4.1^*$
<b>(2<i>S</i>,4<i>R</i>)-29</b>			$109.8 \pm 2.29^*$
<b>(2<i>R</i>,4<i>S</i>)-29</b>			$108.7 \pm 7.91$
<b>30</b>			$108.5 \pm 7.41$
<b>31</b>			$109.7 \pm 8.42$
<b>32</b>			$101.0 \pm 5.26$
<b>33</b>			$106.4 \pm 6.75$
<b>34</b>			$110.2 \pm 6.68$

35			118.2 ± 3.61*
36			94.2 ± 2.48
37			117.9 ± 5.90*
(2 <i>S</i> ,4 <i>R</i> )-38			114.7 ± 10.10
(2 <i>R</i> ,4 <i>S</i> )-38			106.7 ± 10.25
(2 <i>R</i> ,4 <i>S</i> )-39			98.9 ± 4.15
(2 <i>S</i> ,4 <i>R</i> )-39			99.3 ± 2.15

Compared to **3**, *in vitro* characterization of **12** displayed a similar increase in the  $E_{\max}$  of 5-HT-induced  $\text{Ca}_i^{2+}$  release in the absence of a leftward shift in the  $\text{EC}_{50}$ , indicating that **12** improved the efficacy of 5-HT without a change in potency for 5-HT at the 5-HT<sub>2C</sub>R. Compound **12** was counter-screened in h5-HT<sub>2A</sub>R-CHO cells and no alteration in the  $E_{\max}$  or  $\text{EC}_{50}$  of 5-HT-induced  $\text{Ca}_i^{2+}$  release was observed (**Table 3**). Likewise, the additional compounds [(**2*R*,4*S***)-**11**, **13**, **14**, **29**, **35**, **37**] that were validated *in vitro* as 5-HT<sub>2C</sub>R PAMs did not significantly alter the  $E_{\max}$  or  $\text{EC}_{50}$  of 5-HT-induced  $\text{Ca}_i^{2+}$  release in h5-HT<sub>2A</sub>R-CHO cells. Thus, the herein identified 5-HT<sub>2C</sub>R PAMs exhibit selectivity against 5-HT<sub>2A</sub>R *in vitro*.

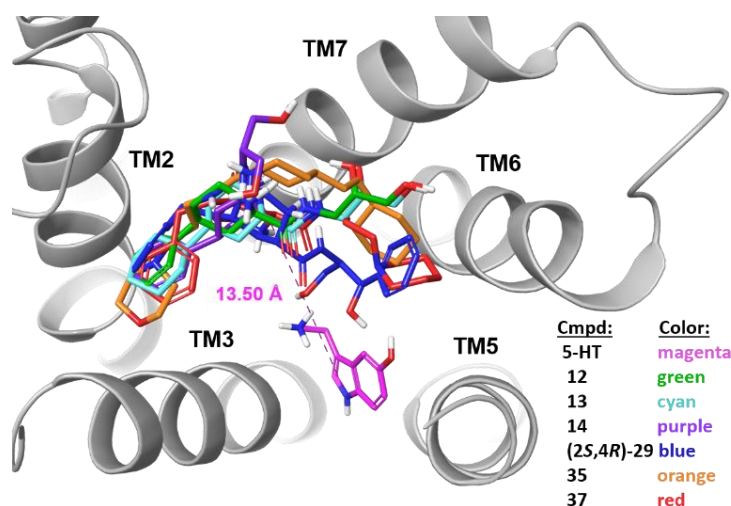
**Table 3. Effects of active 5-HT<sub>2C</sub>R PAMs (1 nM) on 5-HT-induced  $\text{Ca}_i^{2+}$  release in h5-HT<sub>2A</sub>R-CHO cells**

Compound Number	LT	PH	$E_{\max}$ RFU (%5-HT) <sup>a</sup>
(2 <i>R</i> ,4 <i>S</i> )-11			102.6 ± 2.81

12			$103.4 \pm 5.79$
13			$97.8 \pm 2.44$
14			$99.3 \pm 1.58$
29			$103.9 \pm 2.22$
35			$97.2 \pm 4.64$
37			$97.9 \pm 1.99$

**Molecular Modeling and Docking of 5-HT<sub>2c</sub>R PAMs.** The narrow range of the elevated  $E_{\max}$  values resulting from our 5-HT<sub>2c</sub>R PAMs suggests a conserved positive allosteric modulatory mechanism, likely originating from binding to a shared allosteric binding site. To probe possible binding sites the Schrödinger Drug Discovery Suite was used for modeling the 5-HT<sub>2c</sub>R and for docking the 5-HT<sub>2c</sub>R PAM molecules. This effort utilized the recently reported 5-HT<sub>2c</sub>R X-ray crystal structure in complex with the orthosteric agonist ergotamine (PDB: 6BQG).<sup>28</sup> Ergotamine is larger than the 5-HT<sub>2c</sub>R endogenous agonist 5-HT and ergotamine interacts with numerous 5-HT<sub>2c</sub>R residues throughout the transmembrane domains (TM) and extracellular loop 2 (ECL2). In this context, PAM docking protocols are improved due to the stabilization and resultant enhanced atomic resolution in the outer regions of the TM as well as the ECL2. However, to obtain a docking model that is representative of the 5-HT<sub>2c</sub>R conformation encountered by 5-HT<sub>2c</sub>R PAMs *in vitro* and *in vivo*, the Schrodinger Induced Fit Docking (IFD) utility was used to replace ergotamine with 5-HT and allow ligand-induced conformational flexibility. Briefly, the X-ray crystal structure of ergotamine-5-HT<sub>2c</sub>R (PDB: 6BQG) was preprocessed and optimized with the Schrödinger Protein Preparation Wizard using default settings and each ligand (5-HT and 5-HT<sub>2c</sub>R PAMs) was

prepared with the LigPrep tool to generate 3D conformations for docking. Serotonin was docked to the 5-HT<sub>2C</sub>R orthosteric site via IFD with a Glide grid centered on the ergotamine indole N atom and default values for sidechain and residue flexibility. The resultant 5-HT-5-HT<sub>2C</sub>R complex model (**Figure 5**) was checked against published site-directed mutagenesis studies to assess 5-HT orientation accuracy and was subsequently used for the remaining ligand docking.<sup>29</sup>

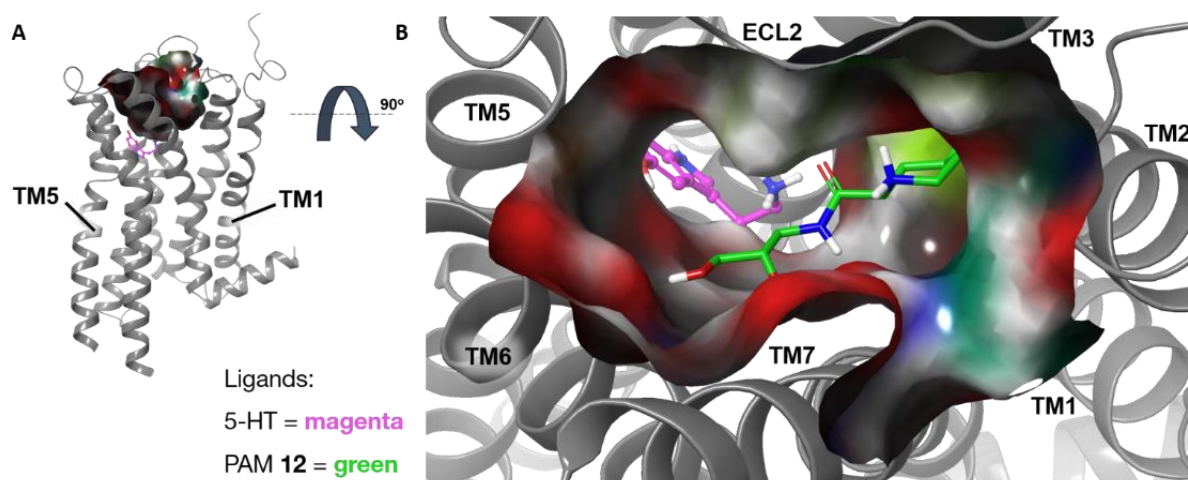


**Figure 5. Molecular docking illustrates the considerable overlap in ligand poses of six 5-HT<sub>2C</sub>R PAMs.** Six small molecules with a 5-HT<sub>2C</sub>R PAM profile are represented in different colors along with the endogenous agonist 5-HT. A representative pose for each 5-HT<sub>2C</sub>R PAM was selected rationally from a top-scoring, enriched cluster docked to the 5-HT<sub>2C</sub>R X-ray crystal structure (PDB: 6BQG). A measurement from the 5-HT (magenta) indole N atom to the piperidine core N atom of compound **12** was found to be 13.5 Å (illustrated by the dashed line).

Selected compounds that displayed *in vitro* 5-HT<sub>2C</sub>R PAM functional activity were docked to the 5-HT-5-HT<sub>2C</sub>R complex model using Glide XP precision and IFD without designated exclusion parameters, as the model contained a 5-HT molecule to block the interaction of PAMs with the orthosteric binding site. Scoring functions (GScore) and biological and chemical rationales were used for ligand pose clustering and selection. The result upon docking six PAMs [**12**, **13**, **14**, (**2S,4R**)-**29**, **35**, **37**] to the 5-HT-5-HT<sub>2C</sub>R model is a striking display of conformational



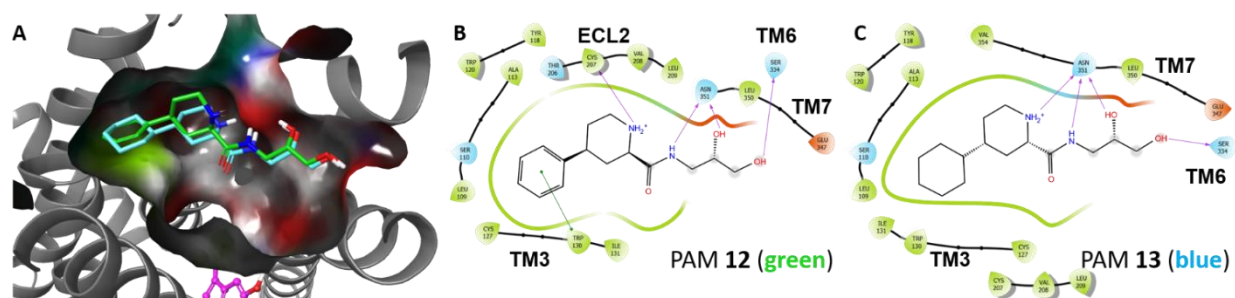
agreement at a spatially distinct allosteric site (**Figure 5**). The distance between the 5-HT indole N-atom and the piperidine ring N-atom from the core of **12** is 13.5 Å. Surface mapping using electrostatics and polarity was used for further docking site characterization with **12**, which shows that the allosteric site is positioned near extracellular-facing regions of the 5-HT<sub>2c</sub>R (**Figure 6A**). Additionally, the PAM orientation reaches across the transmembrane bundle from a lipophilic pocket between TM2 and TM3 towards polar residues located in TM6 and TM7 (**Figure 6B**). Interestingly, the lipophilic and polar surfaces of the docking site correspond to the LT and PH moieties that have been featured in all active 5-HT<sub>2c</sub>R PAMs throughout our discovery and optimization efforts.



**Figure 6. Docking site surface mapping illustrates the distinct location of the proposed allosteric site in relation to 5-HT bound to the 5-HT<sub>2c</sub>R.** (A) The side profile view of 5-HT<sub>2c</sub>R with the protein surface illustrated around the allosteric docking site in the transmembrane helical bundle. 5-HT (magenta) can be seen below the surface illustration. (B) Docking pose of **12** (green) is shown bridging the helical bundle at a site distinct from 5-HT. (5-HT<sub>2c</sub>R PDB: 6BQG)

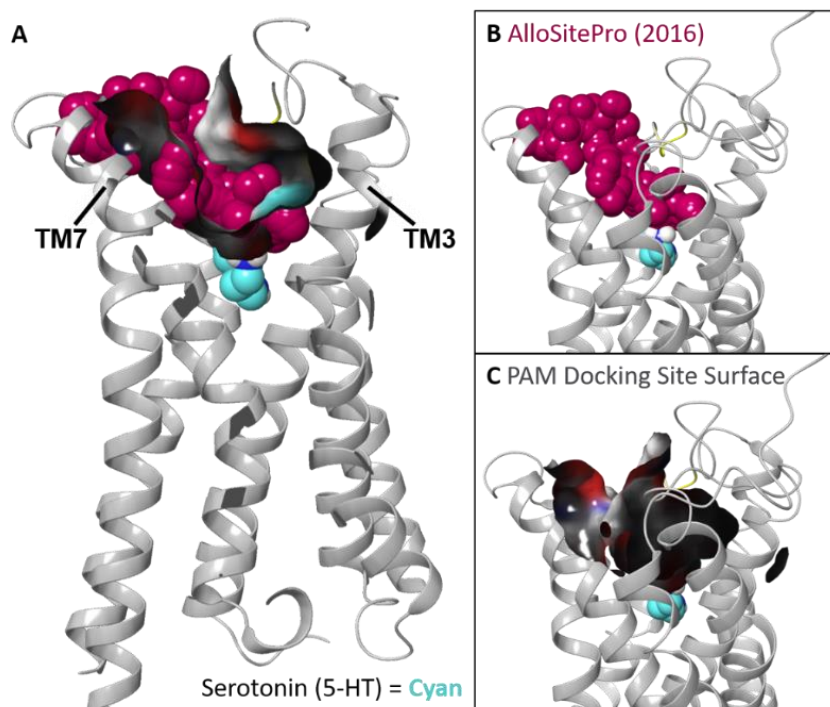
The depth of the lipophilic pocket between TM2 and TM3 drew our attention and likely provides a volume for anchoring the PAM LT. A comparison of docking poses of the 4-phenyl substituted **12** and the 4-cyclohexyl substituted **13** (**Figure 7A**) reveals an aromatic,  $\pi$ - $\pi$  stacking

interaction between **12** and TRP130 located in TM3 (**Figure 7B**), which is not present with the non-aromatic **13** and may prove to be an important feature of the lipophilic pocket. Of note, when viewing compounds **35** and **37** (**Figure 5**), which contain a less polar morpholine PH and differ by an ethylcyclohexyl or phenethyl respectively, the presence of an aromatic interaction between TRP130 and **37** may result in the phenethyl preferentially occupying the lipophilic pocket. Contrarily, **35** is unable to form an aromatic interaction with TRP130 in the lipophilic pocket and results in a flipped pose in which the morpholine occupies the lipophilic pocket. Consistent with our previous docking results for **3**,<sup>23</sup> compound **12** forms contacts with SER334 in TM6 and a residue in the ECL2 (**Figure 7B**). Reducing the length and rotatable bond number in the LT of **12** may have allowed for an optimized binding orientation with the number of molecular contacts increasing accordingly compared to **3**. **Figure 7B** shows the interaction diagram for **12** and includes an aromatic interaction with TRP130 (TM3), an H-bond interaction between the ionizable N atom of the piperidine ring and CYS207 (ECL2), H-bond interactions between the amide NH, 1,2-diol hydroxy group and ASN351 (TM7), and an H-bond interaction between the remaining 1,2-diol hydroxy group and SER334 (TM6). The 4-cyclohexyl substituted **13** (**Figure 7C**) lacks the  $\pi$ - $\pi$  stacking ability of **12** while retaining activity; thus, suggesting the aromatic interaction is not a major contributor to functional activity. Additionally, the piperidine core configuration of **12** (2*R*,4*S*) as docked is notably different than that of **13** (2*S*,4*R*), and, among 5-HT<sub>2c</sub>R PAMs that returned rational poses, there was no consensus for the preferred conformation. Thus, these findings suggest that the piperidine core may not be critical for binding or functional activity once the PH and LT are in favorable positions.



**Figure 7. Docking demonstrates aromatic or aliphatic compact LTs orient towards the hydrophobic pocket between TM2 and TM3 of the 5-HT<sub>2c</sub>R (5-HT<sub>2c</sub>R PDB: 6BQG).** (A) This view features a cutaway of the surface illustration to show how the phenyl and cyclohexyl LTs of **12** (green) and **13** (blue) occupy a hydrophobic pocket within the transmembrane helical bundle. (B) Predicted interactions formed by docking **12** including a possible aromatic interaction with TRP130 in the hydrophobic pocket. (C) Predicted interactions formed by docking **13**.

Following the prediction of a conserved allosteric docking site via the Schrodinger Drug Discovery Suite, an additional *in silico* methodology was employed to predict possible allosteric binding sites on the 5-HT<sub>2c</sub>R without *a priori* PAM structural information. AlloSitePro is a computational tool featuring a support vector machine (SVM) decision engine based on topological and physicochemical properties of the binding pocket.<sup>30</sup> Thus, this methodology provides a ligand-independent allosteric site prediction, whereas by definition, docking provides a ligand-dependent allosteric site prediction. The web-based AlloSitePro was initiated using the ergotamine-5-HT<sub>2c</sub>R complex X-ray crystal structure (PDB: 6BQG). The coordinates for predicted allosteric binding site volumes were translated into magenta-colored sphere representation and superimposed on the molecular docking model (**Figure 8A-B**). When viewed simultaneously, the allosteric docking site surface map and the allosteric site prediction coordinates are highly convergent, providing further support for the described, putative 5-HT<sub>2c</sub>R allosteric site (**Figure 8A**).



**Figure 8. Comparison of the allosteric binding site surface map and an independent allosteric binding site prediction program for the 5-HT<sub>2c</sub>R model (5-HT<sub>2c</sub>R PDB: 6BQG).** (A) Composite model displaying docking site protein surface and predicted allosteric site volume (magenta balls) seen via cutaway to visualize the overlap between the models. (B) The volume (magenta) determined to be a probable binding pocket capable of accommodating an allosteric modulator. (C) From the same angle as panel B, the docking site protein surface is displayed.

***In Vitro* Assessment of Off-target Effects of Compound 12.** To evaluate off-target interactions for a panel of biologically relevant GPCRs and monoamine transporters, **12** was submitted to the National Institute of Mental Health (NIMH) Psychoactive Drug Screening Program (PDSP). At the assessed PAM concentration of 10  $\mu$ M, none of the receptor targets returned inhibition greater than 50%, a level considered above assay noise and indicative of test ligand interaction (**Table 4**). This result improves upon our previously reported compound **3**, (10  $\mu$ M) which exhibited marked inhibition of radioligand binding interactions at the dopamine transporter (DAT; 66.3%), dopamine D3 receptor (71.7%), and  $\alpha$ 2A and  $\alpha$ 2B receptors (85.1% and 80.7%, respectively).<sup>23</sup>

Interestingly, **12** maintains the same 1,2-propanediol moiety in the PH position as **3**, differing only the LT position by replacing the undecyl moiety with a phenyl substituent. The undecyl to phenyl change results in a more compact, aromatic ligand, which could be expected to increase promiscuity among monoamine GPCRs. However, it is likely that the removal of the undecyl moiety reduces nonspecific lipophilic interactions, while the replacement with a phenyl group allows further site-specific interactions to occur, as suggested by molecular modeling. Thus, the selectivity profile of **12** against numerous GPCR orthosteric sites and the comparative analysis vs. **3** provides evidence that the functional allosteric site occupied by **12** is not an evolutionarily residual binding pocket from another orthosteric site. From a development perspective the selectivity profile strongly supports the advancement of **12** towards *in vitro* pharmacokinetic (PK) evaluation and *in vivo* rodent behavioral characterization.

**Table 4. Displacement of radioligand binding by compound 12 (10  $\mu$ M) in a broad panel of receptors and transporters**

Receptor / transporter	Radioligand	% inhibition (10 $\mu$ M) <sup>a</sup>	K <sub>i</sub> ( $\mu$ M) <sup>b</sup>
5-HT <sub>1A</sub>	[ <sup>3</sup> H]-8-OH-DPAT	28.4	NT
5-HT <sub>1B</sub>	[ <sup>3</sup> H]-GR125743	12.3	NT
5-HT <sub>1D</sub>	[ <sup>3</sup> H]-GR125743	15.3	NT
5-HT <sub>1E</sub>	[ <sup>3</sup> H]-5-HT	6.3	NT
5-HT <sub>2A</sub>	[ <sup>3</sup> H]-Ketanserin	-4.3	NT
5-HT <sub>2B</sub>	[ <sup>3</sup> H]-LSD	-7.2	NT
5-HT <sub>2C</sub>	[ <sup>3</sup> H]-Mesulergine	26.9	NT
5-HT <sub>3</sub>	[ <sup>3</sup> H]-LY278584	22.3	NT
5-HT <sub>5A</sub>	[ <sup>3</sup> H]-LSD	-4.3	NT
5-HT <sub>6</sub>	[ <sup>3</sup> H]-LSD	2.5	NT
5-HT <sub>7</sub>	[ <sup>3</sup> H]-LSD	2.2	NT
D <sub>1</sub>	[ <sup>3</sup> H]-SCH23390	9.7	NT
D <sub>2</sub>	[ <sup>3</sup> H]- <i>N</i> -Methylspiperone	7.5	NT
D <sub>3</sub>	[ <sup>3</sup> H]- <i>N</i> -Methylspiperone	19.4	NT
D <sub>4</sub>	[ <sup>3</sup> H]- <i>N</i> -Methylspiperone	-9.3	NT
D <sub>5</sub>	[ <sup>3</sup> H]-SCH23390	9.4	NT
DAT	[ <sup>3</sup> H]-WIN35428	40.8	NT

SERT	[ <sup>3</sup> H]-Citalopram	47.5	NT
NET	[ <sup>3</sup> H]-Nisoxetine	74.4	2.5
α <sub>1A</sub>	[ <sup>3</sup> H]-Prazosin	-16.2	NT
α <sub>1B</sub>	[ <sup>3</sup> H]-Prazosin	-11.0	NT
α <sub>1D</sub>	[ <sup>3</sup> H]-Prazosin	-4.8	NT
α <sub>2A</sub>	[ <sup>3</sup> H]-Rauwolscine	-7.6	NT
α <sub>2B</sub>	[ <sup>3</sup> H]-Rauwolscine	14.5	NT
α <sub>2C</sub>	[ <sup>3</sup> H]-Rauwolscine	-1.8	NT
β <sub>1</sub>	[ <sup>125</sup> I]-Pindolol	-7.7	NT
β <sub>2</sub>	[ <sup>3</sup> H]-CGP12177	-15.9	NT
β <sub>3</sub>	[ <sup>3</sup> H]-CGP12177	-11.2	NT
CB <sub>1</sub>	-	-	NT
CB <sub>2</sub>	[ <sup>3</sup> H]-CP55940	30.6	NT
δOR	[ <sup>3</sup> H]-DADLE	-6.1	NT
κOR	[ <sup>3</sup> H]-U69593	13.4	NT
μOR	[ <sup>3</sup> H]-DAMGO	23.3	NT
GABA <sub>A</sub>	[ <sup>3</sup> H]-Muscimol	7.0	NT

<sup>a</sup> The percent (%) inhibition at multiple targets was tested at 10 μM of compound **12**. Inhibition results > 50% are considered to be a reliable indication that the test compound displaced the radioligand at the target binding site. <sup>b</sup> For inhibition results > 50%, a K<sub>i</sub> value was obtained via a non-linear regression analysis of radioligand competition isotherms. K<sub>i</sub> values were calculated from best fit IC<sub>50</sub> values using the Cheng-Prusoff equation. NT = not tested, The average K<sub>i</sub> from repeated experiments was determined for NET.

***In Vitro and In Vivo Pharmacokinetic (PK) Profiling and In Silico Toxicological Profiling.***

The PK profile of **12** was assessed to determine whether this compound maintained favorable drug-like properties for utility as an *in vivo* probe. Additionally, *in silico* toxicological prediction scoring was used as a cautionary guide before *in vivo* rat behavioral assessments were made. Initially, **12** was subject to a battery of *in vitro* PK assessments, which returned an excellent profile (**Table 5**). In rat liver microsomal fractions spiked with NADPH, clearance (CL<sub>int</sub>) was < 9.6 μL/min mg and the half-life (t<sub>1/2</sub>) was > 240 min. Rat plasma protein binding studies displayed a free (unbound) fraction of 66% for **12**. Compound **12** was highly soluble in physiologically relevant conditions and did not display meaningful inhibition of any cytochrome P450 enzyme tested. In an efflux

substrate assay utilizing a semi-permeable membrane of Madin-Darby Canine Kidney (MDCK) cells expressing the P-glycoprotein (P-gp) efflux protein and the multidrug resistance mutation 1 (MDR1) gene (MDCK-MDR1), compound **12** exhibited a tolerable efflux ratio of 30.9. *In silico* toxicity profiling was performed using the ProTox-II web-based prediction tool and **12** was predicted to belong to a low toxicity class with a high degree of safety predicted for the doses utilized for *in vivo* assessments (below).<sup>31</sup> We also calculated the CNS multiparameter optimization (MPO) value for compound **12** to be 4.7. CNS MPO values range from 0 to 6 with the higher MPO scores predicted to be more desirable for CNS-penetrant medication candidates (**Table S2**).<sup>32</sup> Lastly, the *in vivo* PK profile of **12** was obtained in male Sprague-Dawley rats (**Table 6**) and was observed as overall favorable and in line with our *in vitro* observations (**Table 5**). Specifically, 10 mg/kg of **12** administered iv ( $t_{1/2} = 1.25 \pm 0.02$  h) or 20 mg/kg administered po ( $t_{1/2} = 4.4 \pm 0.5$  h) resulted in appropriate blood plasma concentrations (**Table 6**). The brain concentrations of **12** administered at 10 mg/kg iv were  $96.4 \pm 7.2$  ng/g at 15 min and  $94.0 \pm 1.3$  ng/g at 1 hr. The brain-to-plasma ratios at 10 mg/kg iv were  $0.07 \pm 0.0012$  (15 min) and  $0.11 \pm 0.0056$  (1 hr). Brain-to-plasma concentration ratios  $>0.04$  are consistent with CNS penetration.<sup>33</sup> These cumulative findings suggested that compound **12** would have adequate target exposure for *in vivo* rat behavioral assessments.

**Table 5. *In Vitro* Pharmacokinetic Profile and *In Silico* Toxicity Prediction for Compound **12**<sup>a</sup>**

Compound 12			
<i>In Vitro</i> Pharmacokinetics		<i>In Silico</i> Toxicity (ProTox-II)	
Rat Liver Microsomal Clearance (NADPH)	$CL_{int} = <9.6 \mu\text{L}/\text{min mg}$ $t_{1/2} = >240 \text{ min}$	Predicted LD <sub>50</sub>	3990 mg/kg
Rat Plasma Protein Binding	$F_{uplasma} = 66\%$	Toxicity Class 1-6 (1 = high, 6 = low)	5
CYP3A4 Inhibition	0.0% (10 $\mu\text{M}$ )	Prediction Accuracy	69.26%

CYP2C9 Inhibition	0.0% (10 μM)	Organ Toxicity (probability)	Inactive (0.83)
CYP2D6 Inhibition	1.9% (10 μM)	Carcinogenicity (probability)	Inactive (0.71)
CYP2C19 Inhibition	0.0% (10 μM)	Immunotoxicity (probability)	Inactive (0.99)
CYP1A2 Inhibition	11.8% (10 μM)	Mutagenicity (probability)	Inactive (0.66)
Kinetic Solubility (PBS; pH 7.4)	>100 μM (2 hr)	Cytotoxicity (probability)	Inactive (0.76)
MDCK-MDR1 Permeability	$P_{app}^{A \rightarrow B} = 0.04 \cdot 10^{-6}$ cm/s	Aryl hydrocarbon Receptor (probability)	Inactive (0.96)
	$P_{app}^{B \rightarrow A} = 1.3 \cdot 10^{-6}$ cm/s	Estrogen Receptor Alpha (probability)	Inactive (0.90)
	Efflux ratio = 30.9	Androgen Receptor (probability)	Inactive (0.95)

<sup>a</sup>*In vitro* PK included assessment of 10 μM of compound **12** in liver microsomal clearance performed under NADPH-dependent conditions and cytochrome P450 enzymatic inhibition assays performed and represented as percent inhibition. The P-gp efflux substrate experiment employed Madin-Darby Canine Kidney (MDCK) cells expressing multidrug resistance mutation 1 (MDR1) gene. *In silico* toxicity prediction profile shown along with statistical probabilities (more information at [http://tox.charite.de/protox\\_II/](http://tox.charite.de/protox_II/)).<sup>31</sup>

**Table 6. *In Vivo* Pharmacokinetic Profile and Brain Penetrability of Compound **12**<sup>a</sup>**

Pharmacokinetic profile of <b>12</b>							
Dose (mg/kg)	T <sub>1/2</sub> (h)	T <sub>max</sub> (h)	CL (L h <sup>-1</sup> kg <sup>-1</sup> )	V <sub>ss</sub> (L/kg)	C <sub>max</sub> (ng/mL)	AUC <sub>0–inf</sub> (ng·h·mL <sup>-1</sup> )	F (%)
10, iv	1.25 ± 0.02	<i>b</i>	3.28 ± 0.2	5.4 ± 0.3	2408.6 ± 216.8	3065.6 ± 184.7	<i>b</i>
20, po	4.4 ± 0.5	1.3 ± 0.34	10.89 ± 3.5	70.6 ± 23.7	411.3± 105.7	2244.7 ± 667.8	36.3 ± 11
Brain penetration analysis of <b>12</b>							
Dose (mg/kg)	Time (h)	Brain conc. (ng/g)	Plasma conc. (ng/mL)	Brain:Plasma Ratio			
10, iv	0.25	96.4 ± 7.2	1486.5 ± 89.6	0.07 ± 0.001			
10, iv	1.0	94.0 ± 1.3	892.1 ± 39.1	0.11 ± 0.005			
<sup>a</sup> Values are the average of results (± SEM) from male Sprague-Dawley rats (n = 3/treatment group). Vehicle, 10% DMSO:90% 2-hydroxypropyl-β-cyclodextrin (HP-β-CD). T <sub>1/2</sub> , half-life; T <sub>max</sub> , time of maximum concentration; CL, plasma clearance; V <sub>ss</sub> , volume of distribution; C <sub>max</sub> , maximum concentration; AUC <sub>0–inf</sub> , area under the plasma concentration–time curve; <i>F</i> , oral bioavailability; Time, hours after dose for brain collection; Brain conc., averaged concentration of <b>12</b> in tissue sample. <sup>b</sup> Not determined.							

**Analysis of Compound **12** in a Drug Discrimination Assay.** The drug discrimination assay is a powerful *in vivo* tool for establishing the interoceptive (subjective) effects of novel compounds as well as for establishing their mechanisms of action in humans and animals.<sup>23, 34–43</sup> This assay has been employed to reliably characterize the neurobiological profiles of 5-HT<sub>2c</sub>R agonists (i.e., Ro



60-0175, WAY163909) as well as GPCR allosteric modulators.<sup>23, 35, 38-42</sup> In the present series of studies, we trained rats (n=13) to discriminate the selective 5-HT<sub>2c</sub>R agonist WAY163909 [0.75 mg/kg, intraperitoneal (ip); 15 min pretreatment] from an equivalent volume (1 ml/kg) of saline (0.9% NaCl) in a two-lever drug discrimination protocol under a fixed ratio 20 (FR 20) schedule of water reinforcement.<sup>23</sup> In substitution tests, animals were tested for lever selection after the administration of various doses of the training drug WAY163909 or compound **12**. In combination tests, animals were administered **12** (0.5-2 mg/kg) with a dose of WAY163909 (0.5 mg/kg) that produced ~50% WAY163909-appropriate responding when given alone. We also assessed the ability of the selective 5-HT<sub>2c</sub>R antagonist SB242084 to block the substitution of compound **12** *plus* a low dose of WAY163909.<sup>44</sup>

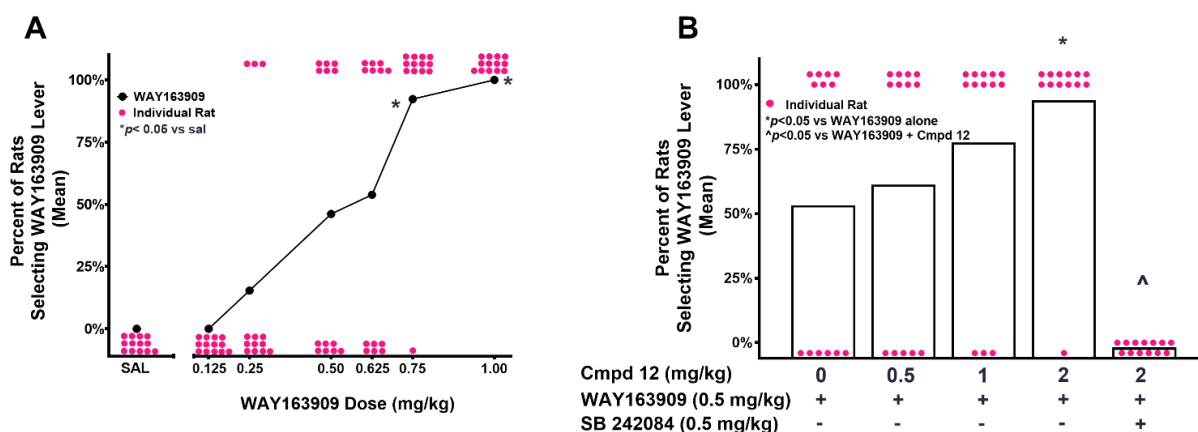
All rats acquired the WAY163909 vs. saline discrimination to criterion. The mean number of sessions required to meet the acquisition criterion (defined as 10 consecutive sessions with  $\geq$  80% of stimulus-appropriate responding) for the WAY163909 vs. saline discrimination was 57 training sessions (range: 39-68). Substitution of a test drug for the training stimulus is typically a quantal rather than continuous function of stimulus similarity in the two-choice drug discrimination assay.<sup>23, 34-42</sup> Thus, intermediate doses of WAY163909 evoke responding confined to one lever. Full substitution was defined as  $\geq$  80% of rats selecting the WAY163909-appropriate lever. Partial substitution was defined as  $\geq$  40% and  $<$  80% drug-appropriate responding. As can be seen in **Figure 9A**, 0% of rats (0/13 rats) chose the WAY163909-associated lever when administered saline or 0.125 mg/kg, while 92% (12/13 rats) and 100% (13/13) of rats chose the WAY163909-associated lever at the training dose (0.75 mg/kg) and 1.0 mg/kg of WAY163909, respectively (vs. saline,  $p < 0.05$ ). Intermediate doses of WAY163909 (0.25-0.625 mg/kg) resulted in a graded, quantal increase in the number of rats selecting the WAY163909-associated lever.

The response rate (responses/min) observed following saline administration was significantly higher than following injection of 0.75 mg/kg ( $t_{12} = 2.22$ ,  $p < 0.05$ ) and 1.0 mg/kg of WAY163909 ( $t_{12} = 3.74$ ,  $p < 0.05$ ). The response rates analyzed for remaining doses of WAY163909 tested (0.125, 0.25, 0.50, 0.625, 1.0 mg/kg, ip) did not differ relative to 0.75 mg/kg of WAY163909 (n.s.). Here, 0.5 and 0.625 mg/kg doses of WAY163909 resulted in 46% and 54% of rats selecting the WAY163909-appropriate lever. Log-probit analyses indicate that the dose of WAY163909 predicted to result in 50% drug-associated responses ( $ED_{50}$ ) is 0.51 mg/kg, in agreement with our previous study (0.53 mg/kg).<sup>23</sup>

Compound **12** did not exhibit intrinsic activity as a 5-HT<sub>2c</sub>R agonist *in vitro* (**Figure 4A**). This result shaped the hypothesis that **12** would fail to substitute in the WAY163909 vs. saline discrimination. As expected from *in vitro* analyses, **12** (0.5 - 5 mg/kg), administered ip 30 min prior to testing, evoked saline-lever responding with no change in response rates (n.s.; **Figure S2**). The observed lack of substitution supports the premise that **12** and the full 5-HT<sub>2c</sub>R agonist WAY163909 have dissociable discriminative stimulus effects.

We next tested the hypothesis that **12** would enhance the discriminative stimulus effects of a subthreshold dose of WAY163909 (0.5 mg/kg). Thus, rats were pretreated with **12** (0, 0.5, 1 or 2 mg/kg) 15 min before WAY163909 (0.5 mg/kg), followed 15 min later by placement in the chambers. **Figure 9B** demonstrates that ~53% of rats (7/13 rats) selected the drug-associated lever following WAY163909 (0.5 mg/kg). Pretreatment with 1 or 2 mg/kg of **12** plus WAY163909 (0.5 mg/kg) evoked ~77% (10/13 rats) and ~92% (12/13 rats) of rats selecting the WAY163909 lever, respectively, suggesting a synergistic substitution for the training drug (**Figure 9B**). The selective 5-HT<sub>2c</sub>R antagonist SB242084 completely reversed the substitution of **12** (2 mg/kg) plus

WAY163909 (0.5 mg/kg) in 13/13 rats. In summary, **12** did not evoke intrinsic 5-HT<sub>2c</sub>R agonist actions, but potentiated a behavioral marker associated with 5-HT<sub>2c</sub>R agonist-mediated signaling *in vivo*.



**Figure 9. Compound 12 dose-dependently augments the stimulus effects of the selective 5-HT<sub>2c</sub>R agonist WAY163909.** (A) The dose-response relationship for WAY163909 is shown ( $n = 13$  rats). Filled magenta circles denote the rats that chose either the saline- or WAY163909-associated lever for each condition/dose. Closed black circles denote the mean percentage of rats selecting the WAY163909-associated lever (Y-axis) [ $*p < 0.05$  vs. saline (SAL)]. (B) Compound (Cmpd) **12** (0-2 mg/kg) or WAY163909 (0.5 mg/kg) was administered alone or combination as illustrated, with or without pretreatment with SB242084 (0.5 mg/kg). Open bars illustrate the mean percentage of rats selecting the WAY163909-associated lever during combination tests (Y-axis) [ $*p < 0.05$  vs. WAY163909 (0.5 mg/kg) alone;  $^{\wedge}p < 0.05$  vs. combination of compound **12** plus WAY163909 following pretreatment with SB242084 (0.5 mg/kg)]. The details of the statistical analyses are found in the Methods section.

## Conclusions

A series of structurally optimized analogues was rationally designed and synthesized based on the scaffold of our previously reported 5-HT<sub>2c</sub>R PAM CYD-1-79 (**3**), bearing privileged diol PH moieties. Specifically, the reported investigation focused on the replacement of the undecyl LT moiety with hydrocarbon fragments (cyclic in nature) with a decreased length while approximately maintaining a similar molecular volume to maintain activity and improve drug-

likeness. Compound **12** (CTW0415) displayed significant PAM activity at the 5-HT<sub>2c</sub>R using a fluorescence-based, 5-HT-evoked Ca<sup>2+</sup> release assay and was shown to be inactive as an agonist or allosteric modulator at the 5-HT<sub>2a</sub>R. An additional six compounds were characterized as 5-HT<sub>2c</sub>R PAMs, enriching our computational molecular modelling studies by providing an interesting array of chemical diversity. The molecular modelling and docking studies provide compelling support for a unique, spatially distinct 5-HT<sub>2c</sub>R allosteric binding site that bridges a hydrophobic pocket between the TM2 and TM3 helices to polar contacts on the TM6 and TM7 helices. One aspect to consider regarding the location of the suggested allosteric site is the evidence of metastable binding sites within transmembrane helical bundles that can briefly accommodate orthosteric ligands.<sup>45-47</sup> The transient nature of these binding pockets may provide a site or a portion of a binding site for specific allosteric modulators to exert negative or positive effects. Future computational and pharmacological experiments are needed to address these ideas.

Compound **12** was ultimately chosen for progression towards *in vivo* behavioral studies due to superior physicochemical properties, an appropriate MPO value, highly selective off-target profile, and promising pharmacokinetics. Moreover, the structure of **12** lends itself to additional medicinal chemistry efforts as the compound is well within the boundaries of Lipinski's Rule of Five. Compound **12** dose-dependently potentiated the stimulus effects of the 5-HT<sub>2c</sub>R agonist WAY163909. Importantly, this effect was completely blocked by the 5-HT<sub>2c</sub>R antagonist SB242084, supporting the critical involvement in the synergism between **12** and a selective 5-HT<sub>2c</sub>R agonist *in vivo*. Taken together, **12** is an ideal lead compound for further optimization as a 5-HT<sub>2c</sub>R PAM and the continued development of this class of molecules may be aided by the structural presentation of a putative 5-HT<sub>2c</sub>R allosteric binding site.

## EXPERIMENTAL SECTION

### Chemistry

**General.** All commercially available starting materials and solvents were reagent grade and used without further purification. Reactions were performed under a nitrogen atmosphere in dry glassware with magnetic stirring. Preparative column chromatography was performed using silica gel 60, particle size 0.063-0.200 mm (70-230 mesh, flash). Analytical TLC was carried out employing silica gel 60 F254 plates (Merck, Darmstadt). Visualization of the developed chromatograms was performed with detection by UV (254 nm). NMR spectra were recorded on a Bruker-600 ( $^1\text{H}$ , 600 MHz;  $^{13}\text{C}$ , 150 MHz) spectrometer or Bruker-300 ( $^1\text{H}$ , 300 MHz;  $^{13}\text{C}$ , 75 MHz).  $^1\text{H}$  and  $^{13}\text{C}$  NMR spectra were recorded with TMS as an internal reference. Chemical shifts were expressed in ppm, and  $J$  values were given in Hz. High-resolution mass spectra (HRMS) were obtained from Thermo Fisher LTQ Orbitrap Elite mass spectrometer. Parameters include the following: Nano ESI spray voltage was 1.8 kV; Capillary temperature was 275 °C and the resolution was 60,000; Ionization was achieved by positive mode. Melting points were measured on a Thermo Scientific Electrothermal Digital Melting Point Apparatus and uncorrected. The purity of final compounds was determined by analytical HPLC using a Shimadzu HPLC system (model: CBM-20A LC-20AD SPD-20A UV/VIS). HPLC analysis conditions: Waters  $\mu$ Bondapak C18 (300  $\times$  3.9 mm); flow rate 0.5 mL/min; UV detection at 270 and 254 nm; linear gradient from 10% acetonitrile in water to 100% acetonitrile in water in 20 min followed by 30 min of the last-named solvent (0.1% TFA was added into both acetonitrile and water). All biologically evaluated

compounds have been characterized with  $^1\text{H}$  NMR,  $^{13}\text{C}$  NMR, HRMS, and HPLC analyses for a quality control to ensure a purity of > 95%.

### General procedure for the synthesis of **11-17**

To a solution of **9** or **10** (0.18 mmol) and amino alcohols (0.18 mmol) in 4 mL of DMF was added HBTU (0.23 mmol) and DIPEA (0.45 mmol). The resulting mixture was stirred at room temperature for 16 h. The DMF was removed under vacuum to give a brown oily residue, which was partitioned between  $\text{CH}_2\text{Cl}_2$  (50 mL) and 10% citric aqueous solution (10 mL). The organic layer was separated and washed with saturated aqueous  $\text{NaHCO}_3$  (10 mL). After drying over anhydrous  $\text{Na}_2\text{SO}_4$ , the solvent was removed under vacuum to give an oily residue. This residue was purified with a silica gel column (5% MeOH in  $\text{CH}_2\text{Cl}_2$ ) and afforded the corresponding Boc-protected amide. The amide (0.13 mmol) was dissolved in  $\text{CH}_2\text{Cl}_2$  (1 mL), followed by the addition of TFA (250  $\mu\text{L}$ ). The resulting mixture was stirred at room temperature. After 2 h, TLC showed that the starting material had disappeared. The solvent was removed under vacuum to give an oily residue. The residue was partitioned between  $\text{CH}_2\text{Cl}_2$  (30 mL) and saturated  $\text{NaHCO}_3$  aqueous solution (10 mL). The organic layer was dried over anhydrous  $\text{Na}_2\text{SO}_4$ , filtered, and concentrated to give an oily residue. This residue was purified with a silica gel column (eluting with 10% MeOH in  $\text{CH}_2\text{Cl}_2$ ), affording compound **11-17**.

**(2*S*,4*S*)-*N*-((1*S*,2*S*)-1,3-Dihydroxy-1-phenylpropan-2-yl)-4-phenylpiperidine-2-carboxamide ((2*S*,4*S*)-11)** and **(2*S*,4*R*)-*N*-((1*S*,2*S*)-1,3-dihydroxy-1-phenylpropan-2-yl)-4-phenylpiperidine-2-carboxamide ((2*S*,4*R*)-11)**.<sup>48</sup> Compounds **(2*R*,4*S*)-11** (36 mg, 40%) and **(2*S*,4*R*)-11** (38 mg, 43%) were prepared from **9** (2 steps), respectively. These two isomers could be separated by preparative TLC as colorless amorphous gel. Compound **(2*R*,4*S*)-11**:  $^1\text{H}$  NMR (600 MHz,  $\text{CDCl}_3$ )  $\delta$  7.42 (m, 2H), 7.30 (m, 4H), 7.22 (m, 2H), 7.12 (d, 2H,  $J = 7.2$  Hz), 5.06 (d,

1H,  $J = 4.2$  Hz), 4.12 (m, 1H), 3.80 (m, 1H), 3.72 (m, 1H), 3.25 (dd, 1H,  $J = 3.0$  Hz, 12.0 Hz), 3.10 (d, 1H,  $J = 12.0$  Hz), 2.65 (m, 1H), 2.55 (m, 1H), 1.95 (d, 1H,  $J = 12.6$  Hz), 1.75 (d, 1H,  $J = 12.6$  Hz), 1.75 (m, 1H), 1.28 (q, 1H,  $J = 12.6$  Hz).  $^{13}\text{C}$  NMR (150 MHz,  $\text{CDCl}_3$ ):  $\delta$  174.5, 145.2, 141.4, 128.4, 128.3 (2C), 127.7, 126.7 (2C), 126.4, 126.1 (2C), 125.9, 73.1, 62.9, 61.0, 56.5, 45.7, 42.0, 37.1, 32.9. HRMS Calcd for  $\text{C}_{21}\text{H}_{26}\text{N}_2\text{O}_3$ :  $[\text{M} + \text{H}]^+$  355.2016; found 355.2022. Compound **(2S,4R)-11**:  $^1\text{H}$  NMR (600 MHz,  $\text{CDCl}_3$ )  $\delta$  7.56 (d, 1H,  $J = 7.8$  Hz), 7.26 (m, 4H), 7.17 (m, 3H), 7.09 (t, 1H,  $J = 7.2$  Hz), 7.04 (d, 1H,  $J = 7.8$  Hz), 4.96 (d, 1H,  $J = 1.8$  Hz), 4.63 (br s, 3H), 4.12 (m, 1H), 3.77 (m, 1H), 3.69 (m, 1H), 3.38 (d, 1H,  $J = 12.0$  Hz), 3.06 (d, 1H,  $J = 10.8$  Hz), 2.59 (m, 1H), 2.54 (m, 1H), 1.87 (d, 1H,  $J = 10.8$  Hz), 1.70 (d, 1H,  $J = 10.8$  Hz), 1.44 (m, 1H), 1.27 (q, 1H,  $J = 13.2$  Hz).  $^{13}\text{C}$  NMR (150 MHz,  $\text{CDCl}_3$ ):  $\delta$  173.2, 144.6, 141.5, 128.5 (2C), 128.2 (2C), 127.5, 126.6 (3C), 125.8 (2C), 72.8, 62.8, 59.8, 56.5, 44.9, 41.3, 36.7, 32.1. HRMS Calcd for  $\text{C}_{21}\text{H}_{26}\text{N}_2\text{O}_3$ :  $[\text{M} + \text{H}]^+$  355.2016; found 355.2019.

**(2,4-cis)-N-((S)-2,3-Dihydroxypropyl)-4-phenylpiperidine-2-carboxamide (12)**: Compound **12** (20 mg, 91%), a diastereomeric mixture, was prepared from **9** (2 steps) as mixture whitish wax.  $^1\text{H}$ -NMR (300 MHz,  $\text{CDCl}_3$ :  $\text{CD}_3\text{OD}$ )  $\delta$  7.43 – 7.23 (m, 2H), 7.22 – 7.12 (m, 3H), 3.77 – 3.61 (m, 1H), 3.57 – 3.40 (m, 2H), 3.40 – 3.07 (m, 8H), 2.92 – 2.58 (m, 2H), 2.28 – 2.06 (m, 1H), 1.92 – 1.75 (m, 1H), 1.68 – 1.40 (m, 2H).  $^{13}\text{C}$  NMR (75 MHz,  $\text{CDCl}_3$ :  $\text{CD}_3\text{OD}$ )  $\delta$  175.0, 174.9, 145.2, 128.5, 126.6, 126.4, 70.6, 70.5, 63.6, 63.5, 60.5, 45.8, 45.7, 42.19, 42.15, 41.8, 41.7, 37.5, 37.4, 33.07, 33.05. HRMS (ESI) calcd for  $\text{C}_{15}\text{H}_{22}\text{N}_2\text{O}_3$   $[\text{M} + \text{H}]^+$  279.1703; found 279.1696.

**((2,4-cis)-4-Cyclohexyl-N-((S)-2,3-dihydroxypropyl)piperidine-2-carboxamide (13)**: Compound **13** (20 mg, 80%), a diastereomeric mixture, was prepared from **10** (2 steps) as a whitish wax.  $^1\text{H}$ -NMR (300 MHz,  $\text{CDCl}_3$ :  $\text{CH}_3\text{OD}$ )  $\delta$  3.80 – 3.48 (m, 5H), 3.42 (d,  $J = 5.3$  Hz, 2H), 3.38

– 3.22 (m, 1H), 3.16 (dd,  $J = 13.7, 6.7$  Hz, 1H), 3.07 (d,  $J = 11.3$  Hz, 1H), 2.53 (t,  $J = 11.3$  Hz, 1H), 1.90 (d,  $J = 12.0$  Hz, 1H), 1.81 – 1.49 (m, 6H), 1.42 – 0.72 (m, 10H).  $^{13}\text{C}$  NMR (75 MHz,  $\text{CDCl}_3 : \text{CD}_3\text{OD}$ )  $\delta$  175.55, 70.48, 63.47, 60.56, 45.71, 42.81, 41.70, 41.40, 33.79, 29.80, 29.30, 26.54, 26.44. HRMS (ESI) calcd for  $\text{C}_{15}\text{H}_{28}\text{N}_2\text{O}_2$   $[\text{M} + \text{H}]^+$  285.2173; found 258.2169.

**(2,4-*cis*)-*N*-(1,3-Dihydroxypropan-2-yl)-4-phenylpiperidine-2-carboxamide (14):** Compound **14** (20 mg, 55.6%), a diastereomeric mixture, was prepared from **9** (2 steps) as mixture whitish wax.  $^1\text{H}$ -NMR (300 MHz,  $\text{CDCl}_3 : \text{CH}_3\text{OD}$ )  $\delta$  7.31 – 7.24 (m, 2H), 7.23 – 7.13 (m, 3H), 3.91 – 3.79 (m, 1H), 3.76 – 3.57 (m, 4H), 3.52 – 3.29 (m, 5H), 3.25 (d,  $J = 12.7$  Hz, 2H), 2.74 (m, 2H), 2.15 (d,  $J = 12.8$  Hz, 1H), 1.84 (d,  $J = 12.8$  Hz, 1H), 1.71 – 1.43 (m, 2H).  $^{13}\text{C}$  NMR (75 MHz,  $\text{CDCl}_3 : \text{CD}_3\text{OD}$ )  $\delta$  173.89, 145.17, 128.53, 126.65, 126.48, 61.80, 61.74, 60.48, 52.32, 45.63, 42.06, 37.25, 32.86. HRMS (ESI) calcd for  $\text{C}_{15}\text{H}_{22}\text{N}_2\text{O}_3$   $[\text{M} + \text{H}]^+$  279.1703; found 279.1700.

**(2,4-*cis*)-4-Cyclohexyl-*N*-(1,3-dihydroxypropan-2-yl)piperidine-2-carboxamide (15):** Compound **15** (5 mg, 36%), a diastereomeric mixture, was prepared from **10** (2 steps) as a whitish wax.  $^1\text{H}$ -NMR (300 MHz,  $\text{CDCl}_3 : \text{CH}_3\text{OD}$ )  $\delta$  3.88 – 3.78 (m, 1H), 3.70 – 3.60 (m, 4H), 3.41 – 3.29 (m, 1H), 3.21 (d,  $J = 12.5$  Hz, 1H), 2.69 (t,  $J = 12.2$  Hz, 1H), 2.02 (d,  $J = 13.0$  Hz, 1H), 1.76 – 1.64 (m, 4H), 1.62 (d,  $J = 12.1$  Hz, 1H), 1.36 – 1.25 (m, 1H), 1.25 – 1.13 (m, 5H), 1.13 – 1.03 (m, 2H), 0.98 – 0.86 (m, 2H).  $^{13}\text{C}$  NMR (75 MHz,  $\text{CDCl}_3 : \text{CD}_3\text{OD}$ )  $\delta$  172.82, 61.79, 60.02, 52.59, 45.12, 42.57, 40.71, 32.69, 29.76, 28.01, 26.50, 26.42. HRMS (ESI) calcd for  $\text{C}_{15}\text{H}_{28}\text{N}_2\text{O}_3$   $[\text{M} + \text{H}]^+$  285.2173; found 285.2169.

**(2,4-*cis*)-*N*-(2-Morpholinoethyl)-4-phenylpiperidine-2-carboxamide (16):** Compound **16** (29 mg, 76%), a diastereomeric mixture, was prepared from **9** (2 steps) as mixture whitish wax.  $^1\text{H}$ -NMR (300 MHz,  $\text{CDCl}_3 : \text{CD}_3\text{OD}$ )  $\delta$  7.39 – 6.87 (m, 5H), 4.01 – 3.72 (m, 7H), 3.75 – 3.44 (m,



5H), 3.29 (d,  $J = 10.9$  Hz, 1H), 2.99 – 2.53 (m, 2H), 2.15 (d,  $J = 11.9$  Hz, 1H), 1.86 (d,  $J = 11.7$  Hz, 1H), 1.64 (dt,  $J = 24.8, 12.5$  Hz, 2H).  $^{13}\text{C}$  NMR (75 MHz,  $\text{CDCl}_3$ )  $\delta$  172.46, 144.44, 128.56, 126.64, 126.55, 61.36, 59.73, 52.63, 41.40, 36.42, 31.62. HRMS (ESI) calcd for  $\text{C}_{18}\text{H}_{27}\text{N}_3\text{O}_2$  [ $\text{M} + \text{H}$ ] $^+$  318.2176; found 318.2190.

**(2,4-*cis*)-4-Cyclohexyl-*N*-(2-morpholinoethyl)piperidine-2-carboxamide (17):** Compound **17** (13 mg, 81%), a diastereomeric mixture, was prepared from **10** (2 steps) as a whitish wax.  $^1\text{H}$ -NMR (300 MHz,  $\text{CDCl}_3$ )  $\delta$  6.94 (s, 1H), 3.75 – 3.68 (m, 4H), 3.37 (q,  $J = 6.0$  Hz, 2H), 3.16 (dd,  $J = 11.4, 2.7$  Hz, 2H), 2.65 (td,  $J = 12.0, 2.6$  Hz, 1H), 2.48 (dd,  $J = 11.8, 5.6$  Hz, 6H), 2.08 (dd,  $J = 12.6, 2.0$  Hz, 1H), 1.92 (s, 1H), 1.81 – 1.54 (m, 6H), 1.31 – 0.78 (m, 9H).  $^{13}\text{C}$  NMR (75 MHz,  $\text{CDCl}_3$ )  $\delta$  174.49, 166.62, 66.96, 61.24, 57.29, 53.43, 46.26, 42.96, 41.62, 35.42, 34.27, 30.05, 29.87, 29.60, 26.70, 26.61. HRMS (ESI) calcd for  $\text{C}_{18}\text{H}_{33}\text{N}_3\text{O}_2$  [ $\text{M} + \text{H}$ ] $^+$  324.2646; found 324.2642.

**(2*S*,4*R*)-*N*-((1*R*,2*R*)-1,3-Dihydroxy-1-phenylpropan-2-yl)-4-phenethylpiperidine-2-carboxamide ((2*S*,4*R*)-29) and (2*R*,4*S*)-*N*-((1*R*,2*R*)-1,3-dihydroxy-1-phenylpropan-2-yl)-4-phenethylpiperidine-2-carboxamide ((2*R*,4*S*)-29).**<sup>48</sup> Compounds **(2*S*,4*R*)-29** (45 mg, 35%) and **(2*R*,4*S*)-29** (50 mg, 39%) were prepared from **25** (2 steps), respectively, by a procedure similar to that used to prepare compound **11**. These two isomers could be separated by preparative TLC as colorless amorphous gels. Compound **(2*S*,4*R*)-29**:  $^1\text{H}$  NMR (600 MHz,  $\text{CDCl}_3$ )  $\delta$  7.54 (br s, 1H), 7.39 (d, 2H,  $J = 7.2$  Hz), 7.32 (m, 2H), 7.26 (m, 3H), 7.17 (m, 3H), 4.91 (d, 1H), 4.12 (dd, 1H,  $J = 5.4$  Hz), 3.64 (dd, 1H,  $J = 5.4$  Hz), 3.51 (dd, 1H,  $J = 5.4$  Hz), 3.48 (m, 1H), 3.25 (m, 1H), 2.76 (m, 1H), 2.63 (t, 2H,  $J = 7.8$  Hz), 2.08 (d, 1H,  $J = 12.6$  Hz), 1.85 (d, 1H,  $J = 13.8$  Hz), 1.26 (m, 1H), 1.16 (q, 1H,  $J = 12.6$  Hz).  $^{13}\text{C}$  NMR (150 MHz,  $\text{CDCl}_3$ ):  $\delta$  171.6, 141.8, 141.5, 128.2, 128.1 (3C),

127.5, 126.1 (2C), 125.7, 72.1, 61.4, 58.9, 57.0, 48.0, 44.1, 38.0, 34.7, 34.2, 32.4, 29.6. HRMS Calcd for  $C_{23}H_{30}N_2O_3$ :  $[M + H]^+$  383.2329; found 383.2332. Compound **(2*R*,4*S*)-29**:  $^1H$  NMR (600 MHz,  $CDCl_3$ )  $\delta$  7.74 (br s, 1H), 7.32 (d, 2H,  $J = 7.8$  Hz), 7.24 (m, 4H), 7.14 (m, 4H), 5.04 (br s, 2H), 4.97 (s, 1H), 4.12 (s, 1H), 3.77 (m, 1H), 3.70 (m, 1H), 3.38 (s, 2H), 3.34 (m, 1H), 3.02 (d, 1H,  $J = 9.6$  Hz), 2.50 (m, 3H), 1.72 (d, 1H,  $J = 10.2$  Hz), 1.61 (d, 1H,  $J = 10.2$  Hz), 1.39 (m, 2H), 1.01 (m, 1H), 0.81 (m, 1H).  $^{13}C$  NMR (150 MHz,  $CDCl_3$ ):  $\delta$  172.2, 142.0, 141.6, 128.4 (2C), 128.2 (2C), 127.4, 125.9 (3C), 72.6, 62.7, 59.1, 56.6, 50.4, 44.2, 38.2, 35.1, 34.3, 32.5, 30.2. HRMS Calcd for  $C_{23}H_{30}N_2O_3$ :  $[M + H]^+$  383.2329; found 383.2334.

**(2,4-*cis*)-*N*-((*S*)-2,3-Dihydroxypropyl)-4-phenethylpiperidine-2-carboxamide (30):**

Compound **30** (20.0 mg, 55.4%), a diastereomeric mixture, was prepared from **25** (2 steps) by a procedure similar to that used to prepare compound **11**, as a white solid. mp 103.2-104.3 °C;  $^1H$ -NMR (300 MHz,  $CDCl_3$  :  $CD_3OD$ )  $\delta$  7.41 – 7.31 (m, 1H), 7.31 – 7.23 (m, 2H), 7.22 – 7.10 (m, 3H), 3.80 – 3.71 (m, 1H), 3.62 – 3.46 (m, 2H), 3.45 – 3.27 (m, 3H), 3.22 (dd, 2H,  $J = 11.6, 2.7$  Hz), 3.18 – 3.09 (m, 1H), 2.62 (t, 3H,  $J = 8.0$  Hz), 2.10 (d, 1H,  $J = 13.2$  Hz), 1.73 (d, 1H,  $J = 13.3$  Hz), 1.56 (q, 2H,  $J = 7.6, 7.2$  Hz), 1.50 – 1.39 (m, 1H), 1.26 (s, 1H), 1.17 – 0.96 (m, 2H)  $^{13}C$  NMR (75 MHz,  $CDCl_3$ )  $\delta$  175.5, 166.6, 142.3, 128.4, 128.3, 125.8, 70.9, 63.8, 63.7, 60.5, 45.6, 42.0, 38.7, 36.7, 35.5, 35.4, 32.7, 32.4. HRMS (ESI) calcd for  $C_{17}H_{26}N_2O_3$   $[M + H]^+$  307.2016; found 307.2009

**(2,4-*cis*)-4-(2-Cyclohexylethyl)-*N*-((*S*)-2,3-dihydroxypropyl)piperidine-2-carboxamide (31):**

Compound **31** (44 mg, 94%), a diastereomeric mixture, was prepared from **26** (2 steps) by a procedure similar to that used to prepare compound **11**, as a whitish wax.  $^1H$ -NMR (300 MHz,  $CDCl_3$ )  $\delta$  7.44 (s, 1H), 3.90 – 3.66 (m, 4H), 3.62 – 3.42 (m, 2H), 3.44 – 3.30 (m, 2H), 3.30 – 3.17

(m, 1H), 3.13 (d, 1H,  $J = 12.0$  Hz), 2.63 (t, 1H,  $J = 12.1$  Hz), 2.02 (d, 1H,  $J = 12.5$  Hz), 1.68 (d, 6H,  $J = 11.4$  Hz), 1.37 (bs, 1H), 1.30 – 1.08 (m, 8H), 1.00 (t, 2H,  $J = 12.3$  Hz), 0.94 – 0.77 (m, 2H).  $^{13}\text{C}$  NMR (75 MHz,  $\text{CDCl}_3$ )  $\delta$  175.3, 70.9, 70.8, 63.8, 63.7, 60.5, 45.6, 42.0, 37.8, 36.8, 36.2, 36.1, 34.2, 33.4, 32.5, 26.7, 26.4. HRMS (ESI) calcd for  $\text{C}_{17}\text{H}_{32}\text{N}_2\text{O}_3$   $[\text{M} + \text{H}]^+$  313.2486; found 313.2486.

**(2,4-*cis*)-*N*-(1,3-Dihydroxypropan-2-yl)-4-phenethylpiperidine-2-carboxamide (32):**

Compound **32** (27 mg, 99%), a diastereomeric mixture, was prepared from **25** (2 steps) by a procedure similar to that used to prepare compound **11**, as a white wax-like material.  $^1\text{H}$ -NMR (300 MHz,  $\text{CDCl}_3$ :  $\text{CD}_3\text{OD}$ )  $\delta$  7.24 – 7.15 (m, 2H), 7.13 – 7.04 (m, 3H), 3.99 (s, 7H), 3.88 – 3.76 (m, 1H), 3.37 (d, 1H,  $J = 10.5$  Hz), 3.18 (d, 1H,  $J = 11.7$  Hz), 2.82 – 2.61 (m, 1H), 2.60 – 2.50 (m, 2H), 2.04 (d, 1H,  $J = 12.6$  Hz), 1.75 (d, 1H,  $J = 12.6$  Hz), 1.66 – 1.37 (m, 3H), 1.33 – 0.97 (m, 3H).  $^{13}\text{C}$  NMR (75 MHz,  $\text{CDCl}_3$ :  $\text{CD}_3\text{OD}$ )  $\delta$  172.1, 141.9, 128.3, 128.1, 125.7, 61.2, 59.3, 52.7, 44.5, 38.2, 35.0, 34.5, 32.4, 30.3. HRMS (ESI) calcd for  $\text{C}_{17}\text{H}_{26}\text{N}_2\text{O}_3$   $[\text{M} + \text{H}]^+$  307.2016; found 307.2012.

**(2,4-*cis*)-4-(2-Cyclohexylethyl)-*N*-(1,3-dihydroxypropan-2-yl)piperidine-2-carboxamide**

**(33):** Compound **33** (20.7 mg, 76.6%), a diastereomeric mixture, was prepared from **26** (2 steps) by a procedure similar to that used to prepare compound **11**, as a whitish solid. mp 145.2-150.0 °C.  $^1\text{H}$ -NMR (300 MHz,  $\text{CDCl}_3$ :  $\text{CD}_3\text{OD}$ )  $\delta$  3.86 (t, 1H,  $J = 4.8$  Hz), 3.80 – 3.57 (m, 4H), 3.48 – 3.33 (m, 1H), 3.23 – 3.06 (m, 2H), 2.70 – 2.54 (m, 1H), 2.00 (d, 1H,  $J = 13.1$ ), 1.75 – 1.60 (m, 6H), 1.38 (bs, 2OH), 1.33 – 1.06 (m, 9H), 1.09 – 0.96 (m, 2H), 0.95 – 0.75 (m, 3H).  $^{13}\text{C}$  NMR (75 MHz,  $\text{CDCl}_3$ :  $\text{CD}_3\text{OD}$ )  $\delta$  174.4, 61.8, 61.7, 60.4, 52.2, 45.5, 37.7, 36.5, 36.0, 34.1, 34.0, 33.3, 32.3, 26.6, 26.3. HRMS (ESI) calcd for  $\text{C}_{17}\text{H}_{32}\text{N}_2\text{O}_3$   $[\text{M} + \text{H}]^+$  313.2486; found 313.2487.

**(2,4-*cis*)-4-(2-Cyclohexylethyl)-*N*-(2-morpholinoethyl)piperidine-2-carboxamide (34):**

Compound **34** (43 mg, 93%), a diastereomeric mixture, was prepared from **26** (2 steps) by a procedure similar to that used to prepare compound **11**, as a yellowish solid. mp 45.0-47.1 °C; <sup>1</sup>H-NMR (300 MHz, CDCl<sub>3</sub>) δ 6.93 (t, 1H, *J* = 5.5 Hz), 3.80 – 3.59 (m, 4H), 3.35 (dtd, 2H, *J* = 6.7, 5.6, 5.0, 1.2 Hz), 3.14 (tt, 2H, *J* = 11.9, 2.4 Hz), 2.77 – 2.56 (m, 1H), 2.56 – 2.37 (m, 6H), 2.18 – 2.03 (m, 1H), 1.95 (d, 1H, *J* = 9.0 Hz), 1.82 – 1.58 (m, 6H), 1.40 – 1.30 (m, 1H), 1.34 – 1.08 (m, 8H), 1.08 – 0.96 (m, 1H), 0.96 – 0.74 (m, 3H). <sup>13</sup>C NMR (75 MHz, CDCl<sub>3</sub> : CD<sub>3</sub>OD) δ 174.3, 67.0, 57.3, 53.4, 46.0, 37.8, 37.2, 36.3, 35.4, 34.2, 33.4, 32.8, 26.7, 26.4. HRMS (ESI) calcd for C<sub>20</sub>H<sub>37</sub>N<sub>3</sub>O<sub>2</sub> [M + H]<sup>+</sup> 352.2959; found 352.2952.

**(2,4-*cis*)-4-(2-Cyclohexylethyl)-*N*-(3-morpholinopropyl)piperidine-2-carboxamide (35):**

Compound **35** (33 mg, 99%), a diastereomeric mixture, was prepared from **26** (2 steps) by a procedure similar to that used to prepare compound **11**, as a white wax-like solid. <sup>1</sup>H-NMR (300 MHz, CDCl<sub>3</sub>) δ 7.51 (t, 1H, *J* = 5.5 Hz), 3.74 (td, 4H, *J* = 4.4, 1.5 Hz), 3.33 (m, 2H), 3.13 (m, 2H), 2.66 (td, 1H, *J* = 12.1, 2.7 Hz), 2.43 (m, 6H), 2.09 (dq, 1H, *J* = 12.8, 2.7 Hz), 1.81 (s, 1H), 1.67 (m, 8H), 1.35 (m, 1H), 1.19 (m, 8H), 1.03 (m, 1H), 0.86 (m, 3H). HRMS (ESI) calcd for C<sub>21</sub>H<sub>39</sub>N<sub>3</sub>O<sub>2</sub> [M + H]<sup>+</sup> 366.3115; found 366.3112.

**(2,4-*cis*)-*N*-(2-morpholinoethyl)-4-phenethylpiperidine-2-carboxamide (36):** Compound **36**

(45 mg, 96%), a diastereomeric mixture, was prepared from **25** (2 steps) by a procedure similar to that used to prepare compound **11**, as a yellowish solid. mp 156.6-157.9 °C; <sup>1</sup>H-NMR (300 MHz, CDCl<sub>3</sub>) δ 7.31 – 7.24 (m, 2H), 7.12 – 7.13 (m, 3H), 6.94 (t, 1H, *J* = 5.6 Hz), 3.71 (t, 4H, *J* = 3.0 Hz), 3.36 (q, 2H, *J* = 6.0 Hz), 3.23 – 3.08 (m, 2H), 2.72 – 2.59 (m, 3H), 2.53 – 2.39 (m, 6H), 2.17 (dq, 1H, *J* = 12.7, 2.8 Hz), 1.73 (dt, 1H, *J* = 12.8, 2.8 Hz), 1.64 – 1.52 (m, 2H), 1.51 – 1.39 (m,

1H), 1.25 (bs, 1H), 1.18 – 1.04 (m, 1H), 1.03 – 0.91 (m, 1H). <sup>13</sup>C NMR (75 MHz, CDCl<sub>3</sub>) δ 174.2, 166.7, 142.5, 128.3, 128.3, 125.7, 67.0, 60.8, 57.3, 53.4, 45.9, 38.9, 35.6, 35.4, 32.8, 32.6. HRMS (ESI) calcd for C<sub>20</sub>H<sub>31</sub>N<sub>3</sub>O<sub>2</sub> [M + H]<sup>+</sup> 346.2489; found 346.2482.

**(2,4-*cis*)-N-(3-morpholinopropyl)-4-phenethylpiperidine-2-carboxamide (37):** Compound **37** (25 mg, 99%), a diastereomeric mixture, was prepared from **25** (2 steps) by a procedure similar to that used to prepare compound **11**, as a white solid. mp 59.8-61.5 °C;. <sup>1</sup>H-NMR (300 MHz, CDCl<sub>3</sub>) δ 7.53 (t, 1H, *J* = 5.2 Hz), 7.27 (m, 2H), 7.17 (m, 3H), 3.74 (dt, 4H, *J* = 4.4, 1.5 Hz), 3.34 (m, 2H), 3.14 (m, 2H), 2.64 (m, 3H), 2.43 (m, 6H), 2.18 (dq, 1H, *J* = 12.6, 2.8 Hz), 1.69 (m, 4H), 1.56 (m, 2H), 1.46 (m, 1H), 1.09 (ddd, 1H, *J* = 15, 12, 3 Hz), 0.96 (q, 1H, *J* = 12 Hz). <sup>13</sup>C NMR (75 MHz, CDCl<sub>3</sub>) δ 174.2, 142.4, 128.3, 128.2, 125.7, 66.9, 61.0, 57.7, 53.8, 45.9, 38.9, 38.6, 37.1, 35.7, 32.8, 32.6, 25.4. HRMS (ESI) calcd for C<sub>21</sub>H<sub>33</sub>N<sub>3</sub>O<sub>2</sub> [M + H]<sup>+</sup> 360.2646; found 360.2638.

**(2*S*,4*R*)-4-(4-(*tert*-Butyl)phenethyl)-N-((1*R*,2*R*)-1,3-dihydroxy-1-phenylpropan-2-yl)piperidine-2-carboxamide ((2*S*,4*R*)-38) and (2*R*,4*S*)-4-(4-(*tert*-butyl)phenethyl)-N-((1*R*,2*R*)-1,3-dihydroxy-1-phenylpropan-2-yl)piperidine-2-carboxamide ((2*R*,4*S*)-38).<sup>48</sup>**

Compounds **(2*S*,4*R*)-38** (40 mg, 28%) and **(2*R*,4*S*)-38** (50 mg, 36%) were prepared from **27** (2 steps), respectively, by a procedure similar to that used to prepare compound **11**. These two isomers could be separated by preparative TLC as colorless amorphous gels. Compound **(2*S*,4*R*)-38**: <sup>1</sup>H NMR (600 MHz, CDCl<sub>3</sub> + CD<sub>3</sub>OD) δ 7.46 (br s, 1H), 7.39 (d, 2H, *J* = 7.2 Hz), 7.31 (m, 4H), 7.24 (t, 1H, *J* = 7.2 Hz), 7.10 (d, 1H, *J* = 8.4 Hz), 4.96 (d, 1H, *J* = 4.8 Hz), 4.09 (q, 1H, *J* = 5.4 Hz), 3.68 (m, 1H), 3.57 (m, 1H), 3.21 (dd, 1H, *J* = 3.0 Hz, 12.0 Hz), 3.12 (m, 1H), 2.63 (m, 1H), 2.57 (t, 2H, *J* = 7.8 Hz), 1.91 (d, 1H, *J* = 13.2 Hz), 1.76 (d, 1H, *J* = 12.6 Hz), 1.54 (m, 2H), 1.46 (m, 1H), 1.30 (s, 9H), 1.12 (qd, 1H, *J* = 3.6 Hz, 12.0 Hz), 0.91 (q, 1H, *J* = 12.6 Hz). <sup>13</sup>C NMR

(150 MHz, CDCl<sub>3</sub> + CD<sub>3</sub>OD):  $\delta$  174.0, 148.5, 141.6, 139.0, 128.1 (2C), 127.8 (2C), 127.4, 126.0, 125.9, 125.1 (2C), 72.0, 61.8, 59.9, 56.6, 44.9, 38.5, 35.8, 34.9, 34.2, 31.9, 31.3, 31.1 (3C). HRMS Calcd for C<sub>27</sub>H<sub>38</sub>N<sub>2</sub>O<sub>3</sub>: [M + H]<sup>+</sup> 439.2950; found 439.2957. Compound **(2R,4S)-38**: <sup>1</sup>H NMR (600 MHz, CDCl<sub>3</sub> + CD<sub>3</sub>OD)  $\delta$  7.68 (br s, 1H), 7.38 (d, 2H, *J* = 7.8 Hz), 7.31 (m, 4H), 7.22 (t, 1H, *J* = 7.2 Hz), 7.11 (d, 2H, *J* = 8.4 Hz), 4.99 (d, 1H, *J* = 4.2 Hz), 4.11 (m, 1H), 3.75 (m, 1H), 3.66 (m, 1H), 3.47 (dd, 1H, *J* = 2.4 Hz, 12.6 Hz), 3.20 (d, 1H, *J* = 11.4 Hz), 2.72 (m, 1H), 2.56 (m, 2H), 1.87 (d, 1H, *J* = 13.2 Hz), 1.78 (d, 1H, *J* = 13.8 Hz), 1.52 (m, 3H), 1.31 (s, 9H), 1.18 (m, 1H), 0.96 (q, 1H, *J* = 12.0 Hz). <sup>13</sup>C NMR (150 MHz, CDCl<sub>3</sub>+CD<sub>3</sub>OD):  $\delta$  171.7, 148.7, 141.5, 138.8, 128.1 (2C), 127.8 (2C), 127.4, 125.9 (2C), 125.2 (2C), 72.4, 62.3, 59.0, 56.6, 44.2, 38.2, 34.8, 34.2, 31.9, 31.3 (4C), 30.1. HRMS Calcd for C<sub>27</sub>H<sub>38</sub>N<sub>2</sub>O<sub>3</sub>: [M + H]<sup>+</sup> 439.2950; found 439.2955.

**(2R,4S)-N-((1S,2S)-1,3-Dihydroxy-1-phenylpropan-2-yl)-4-(4-methylphenethyl)piperidine-2-carboxamide ((2R,4S)-39) and (2S,4R)-N-((1S,2S)-1,3-dihydroxy-1-phenylpropan-2-yl)-4-(4-methylphenethyl)piperidine-2-carboxamide ((2S,4R)-39).**<sup>48</sup> Compounds **(2R,4S)-39** (50 mg, 34%) and **(2S,4R)-39** (53 mg, 37%) were prepared from **28** (2 steps), respectively, by a procedure similar to that used to prepare compound **11**. These two isomers could be separated by preparative TLC as colorless amorphous gels. Compound **(2R,4S)-39**: <sup>1</sup>H NMR (600 MHz, CDCl<sub>3</sub> + CD<sub>3</sub>OD)  $\delta$  7.46 (br s, 1H), 7.39 (d, 2H, *J* = 7.8 Hz), 7.31 (t, 2H, *J* = 7.8 Hz), 7.25 (t, 1H, *J* = 7.2 Hz), 7.09 (d, 2H, *J* = 8.4 Hz), 7.05 (d, 2H, *J* = 7.8 Hz), 4.97 (d, 1H, *J* = 4.2 Hz), 4.08 (d, 1H, *J* = 4.8 Hz), 3.69 (m, 1H), 3.58 (m, 1H), 3.15 (dd, 1H, *J* = 3.0 Hz, 12.0 Hz), 3.11 (m, 1H), 2.60 (m, 1H), 2.55 (t, 2H, *J* = 7.8 Hz), 2.31 (s, 3H), 1.86 (d, 1H, *J* = 13.2 Hz), 1.73 (d, 1H, *J* = 13.2 Hz), 1.50 (m, 2H), 1.42 (m, 1H), 1.09 (dq, 1H, *J* = 4.2 Hz, 12.6 Hz), 0.86 (q, 1H, *J* = 12.0 Hz). <sup>13</sup>C NMR (150 MHz, CDCl<sub>3</sub> + CD<sub>3</sub>OD):  $\delta$  174.3, 141.6, 139.1, 135.1, 128.9 (2C), 128.1 (2C), 128.0 (2C), 127.4, 126.0 (2C), 72.0, 61.9, 60.0, 56.5, 45.0, 38.6, 36.0, 35.0, 32.0, 31.5, 20.6. HRMS Calcd for C<sub>24</sub>H<sub>32</sub>N<sub>2</sub>O<sub>3</sub>:

[M + H]<sup>+</sup> 397.2486; found 397.2490. Compound (**2S,4R**)-**39**: <sup>1</sup>H NMR (600 MHz, CDCl<sub>3</sub>) δ 7.45 (d, 1H, *J* = 8.4 Hz), 7.35 (d, 2H, *J* = 7.2 Hz), 7.25 (m, 2H), 7.18 (t, 1H, *J* = 7.2 Hz), 7.08 (d, 1H, *J* = 7.8 Hz), 7.02 (d, 1H, *J* = 8.4 Hz), 5.02 (d, 1H, *J* = 3.0 Hz), 4.65 (br s, 3H), 4.10 (m, 1H), 3.78 (m, 1H), 3.71 (m, 1H), 3.13 (d, 1H, *J* = 13.8 Hz), 2.94 (d, 1H, *J* = 12.0 Hz), 2.48 (t, 2H, *J* = 7.8 Hz), 2.41 (m, 1H), 2.31 (s, 3H), 1.74 (d, 1H, *J* = 12.0 Hz), 1.59 (d, 1H, *J* = 12.0 Hz), 1.39 (m, 2H), 1.31 (m, 1H), 0.90 (m, 1H), 0.78 (q, 1H, *J* = 12.6 Hz). <sup>13</sup>C NMR (150 MHz, CDCl<sub>3</sub>): δ 173.5, 141.8, 139.1, 135.2, 129.1 (3C), 128.1 (3C), 127.4, 125.9 (2C), 72.7, 62.9, 59.8, 56.4, 44.7, 38.7, 36.1, 34.8, 32.1, 31.5, 21.0. HRMS Calcd for C<sub>24</sub>H<sub>32</sub>N<sub>2</sub>O<sub>3</sub>: [M + H]<sup>+</sup> 397.2486; found 397.2487.

### ***In silico* Molecular Docking**

Molecular modeling and ligand docking were performed in the Maestro (11.9) workspace using modules (LigPrep, Protein Preparation Wizard, Induced Fit Docking, and Glide) in the Small Molecule Drug Discovery Suite (2019-1, Schrödinger, LLC, New York, NY, 2017). The crystal structure of ergotamine-5-HT<sub>2c</sub>R (PDB Code: 6BQG) was fetched from RCSB PDB bank and was preprocessed and optimized with Schrödinger Protein Preparation Wizard using default settings. All ligands (5-HT and 5-HT<sub>2c</sub>R PAMs) were created with Maestro 2D-sketcher and prepared with LigPrep to generate suitable 3D conformations for docking. Induced Fit Docking was used to dock 5-HT and replace ergotamine. For this initial model generation, a grid was applied via Glide on the ergotamine-5-HT<sub>2c</sub>R structure centering on the indole N atom of ergotamine, as a representation of the orthosteric binding site. A new 5-HT-bound 5-HT<sub>2c</sub>R model was generated in this manner, allowing default flexibility and movement of amino acid residues surrounding the orthosteric site, now accommodating 5-HT. The 5-HT-bound 5-HT<sub>2c</sub>R model was exported as a single protein structure (both 5-HT and protein), and subsequently used for docking of the 5-HT<sub>2c</sub>R PAMs. No exclusion volumes were necessary to apply due to the presence of 5-HT in the

orthosteric site. Compound **12** was pharmacologically validated as a 5-HT<sub>2C</sub>R PAM, thus **12** was docked to the model using the Induced Fit Docking protocol, allowing default residue flexibility. A rationally selected docking pose for **12** was used as a center for a new grid. This grid was applied for the standard docking of remaining ligands, conducted with Glide XP mode. All docked results were viewed in Maestro for visualization and clustering. Scoring functions (GScore) and biological and chemical rationale were used for ligand pose selection. For all ligands that were pharmacologically tested as a mixture of two isomers, both isomers were docked and analyzed. Visualization aids such as the protein surface predictions around the docking site were performed in the Maestro workspace.

## ***In Vitro* Pharmacology**

### **Intracellular Calcium (Ca<sup>2+</sup>) Release Assay in h5-HT<sub>2</sub>R-CHO Cells**

Chinese hamster ovary (CHO) cells stably transfected with the human unedited (INI) h5-HT<sub>2C</sub>R (h5-HT<sub>2C</sub>R-CHO cells) or the human h5-HT<sub>2A</sub>R (h5-HT<sub>2A</sub>R-CHO cells) were the generous gift from Drs. Kelly A. Berg and William P. Clarke (University of Texas Health Science Center, San Antonio). Cells were grown at 37°C, 5% CO<sub>2</sub>, and 85% relative humidity environment in GlutaMax-MEM medium (Invitrogen, Carlsbad, CA) containing 5% fetal bovine serum (Atlanta Biologicals, Atlanta, GA) and 100 µg/mL hygromycin (Mediatech, Manassas, VA) and were passaged when they reached 80% confluency. The Ca<sup>2+</sup> release assay was performed according to our recent publications.<sup>23</sup> Briefly, cells (150 µL; passages 6-16 (FlexStation 3; Molecular Devices) or 30,000 cells/well (FLIPR<sup>TETRA</sup>; Molecular Devices) in black-wall 96-well culture plates with optically clear flat bottoms. To ensure even plating of cells, the source reservoir was frequently agitated or triturated, and plates were maintained on a rotary shaker at low speed for 20 min after



plating and returned to the incubator overnight. Approximately 24 h after plating, the medium was replaced with serum-free (SF) GlutaMax-MEM medium supplemented with 20 nM to 100  $\mu$ M putrescine (Sigma-Aldrich, St. Louis, MO), 20 nM to 100  $\mu$ M progesterone (Sigma-Aldrich), and 1:100 ITS (1000 mg/L human recombinant insulin, 550 mg/L human recombinant transferrin, 0.67 mg/L selenious acid; Corning Inc., Corning, NY) (SF+ medium). Following a 3 h incubation, SF+ medium was replaced with 40  $\mu$ L of Hank's balanced saline solution (HBSS; without  $\text{CaCl}_2$  or  $\text{MgCl}_2$ , pH 7.4) plus 40  $\mu$ L of Calcium 4 dye solution (FLIPR No-wash kit, Molecular Devices, Sunnyvale CA, catalog no R8142) supplemented with 2.5 mM of water-soluble probenecid (Sigma-Aldrich) to inhibit extracellular transport of the dye. Plates were incubated with dye solution for 60 min at 37°C, 15 min at room temperature in the dark. Drug dilutions were prepared at 5x final concentration in 1x HBSS; delivery of compound (20  $\mu$ L/well) was followed 15 min later by 5-HT (10 pM to 10  $\mu$ M; 25  $\mu$ L/well). A baseline was established for each well before addition of the test compound and again before addition of 5-HT. The fluorescence read following the addition of 5-HT was used to assess allosteric modulation of 5-HT-evoked  $\text{Ca}_i^{2+}$  release. Fluorescence was measured using a FlexStation 3 (Molecular Devices) or FLIPR<sup>TETRA</sup> (130 gain, 60% intensity, 0.3 s exposure). For the FlexStation 3, a 17 s baseline was established before addition of compounds following which fluorescence was recorded every 1.7 s for a total 240 s. Maximum peak height was determined by the SoftMax software (Pro 5.4.5) for each well. For the FLIPR<sup>TETRA</sup>, a 10 s baseline was established before addition of compounds following which fluorescence was recorded every 1 s for 120 s following compound or for 360 s following 5-HT. Maximum peak height was determined by ScreenWorks 4.0 software for each well. After the final readings, cells were fixed in 2% paraformaldehyde (Sigma) overnight. The maximum 5-HT-induced  $\text{Ca}_i^{2+}$  release ( $E_{\text{max}}$ ) in the presence of test compound was determined using 4-parameter

nonlinear regression analysis (GraphPad Prism 7.04) and calculated from 4-6 biological replicates, each conducted in technical triplicates. The  $E_{\max}$  for the test compound plus 5-HT was normalized to the  $E_{\max}$  for 5-HT alone. Subsequent *post hoc* comparisons between means for  $E_{\max}$  were made using Welch's unpaired  $t$  test (GraphPad Prism). All statistical analyses were conducted with an experiment-wise error rate of  $\alpha = 0.05$ . All treatment assignments were blinded to investigators who performed *in vitro* assays and endpoint statistical analyses.

### ***In Vivo* Pharmacokinetics and Brain Penetration Analyses**

Male Sprague–Dawley rats ( $n = 3$ /treatment group; Charles River Laboratories) weighing 200–250 g at the beginning of the experiment were housed three per cage in a pathogen-free, temperature (20–26°C) and humidity-controlled (40–70%) environment with a 12 h light-dark cycle and ad libitum access to food and filtered water. Rats were randomly assigned to treatment groups. Vehicle [10% DMSO:90% HP- $\beta$ -CD] or compound **12** dissolved in vehicle was administered to rats intravenously (iv) at 10 mg/kg or *per os* (po) at 20 mg/kg. Blood samples (0.3 mL) were collected from the retro-orbital sinus vein before dosing and at 0.08, 0.25, 0.5, 1.0, 2.0, 4.0, 8.0, and 24 h postdosing for iv administration and 0.25, 0.5, 1.0, 2.0, 4.0, 8.0, and 24 h postdosing for po administration. Blood samples were placed in heparinized tubes and centrifuged at 12,000g for 5 min at 4°C. Brain samples were collected at 0.25 and 1 h postdosing. All samples were stored at –20°C. The concentration of **12** in each sample was analyzed by Sundia MediTech Co., Ltd. The study and the related standard operating procedures (SOPs) were reviewed and approved by Sundia Institutional Animal Care and Use Committee. The Sundia animal facility is approved with yearly inspection by the Shanghai Laboratory Animal Management Committee.

The pharmacokinetic parameters of compound **12** were calculated according to a noncompartmental model using WinNonlin 8.1 (Pharsight Corporation, ver 5.3, Mountain View, CA, USA). The peak concentration ( $C_{\max}$ ) and time of peak concentration ( $T_{\max}$ ) were directly obtained from the plasma concentration–time plot. The elimination rate constant ( $\lambda$ ) was obtained by the least-squares fitted terminal log–linear portion of the slope of the plasma concentration–time profile. The elimination half-life ( $t_{1/2}$ ) was evaluated according to  $0.693/\lambda$ . The area under the plasma concentration–time curve from 0 to time  $t$  ( $AUC_{0-t}$ ) was evaluated using the linear trapezoidal rule and further extrapolated to infinity ( $AUC_{0-\infty}$ ) according to the following equation:  $AUC_{0-\infty} = AUC_{0-t} + C_{\text{last}}/\lambda$ . The pharmacokinetic parameters and brain concentrations are presented as mean  $\pm$  S.E.M. in Table 6. All treatment assignments were blinded to investigators who performed pharmacokinetic assays and endpoint statistical analyses.

### Effects of Compound **12** in a Drug Discrimination Assay

**Drugs.** WAY163909 [(7b-*R*,10a-*R*)-1,2,3,4,8,9,10,10a-octahydro-7b*H*-cyclopenta[*b*][1,4]diazepino[6,7,1*hi*]indole] was a gift from Pfizer, Inc. (New York, NY) and was dissolved in 0.9% NaCl (vehicle employed for comparison to WAY163909). SB242084 [6-chloro-5-methyl-1-[[2-(2-methylpyrid-3-yloxy)pyrid-5-yl]carbamoyl]indoline dihydrochloride; Sigma Chemical Co., St. Louis, MO, USA] was dissolved in saline containing 10 mmol/L citric acid (Sigma Chemical Co.) and 8% 2-hydroxypropyl- $\beta$ -cyclodextrin (Trappsol Hydroxpropyl Beta Cyclodextrin, pharmaceutical grade, Cyclodextrin Technologies Development Inc., High Springs, FL, USA) with the final pH of the solution adjusted to 5.6. SB242084, WAY163909, and compound **12** were injected intraperitoneally (ip) at a volume of 1 mL/kg.

**Animals.** Male Sprague–Dawley rats ( $n = 13$ ; Envigo) weighing 300–325 g (~ 60 days of age) at the beginning of the experiment were housed two per cage in a temperature (21–23°C) and humidity-controlled (45–50%) environment; lighting was maintained under a 12h light–dark cycle (0700–1900 h). Rats were maintained at 80–90% of their free-feeding weights by restricting access to water. Rats received water during daily training sessions (5–6 mL/rat/session), several hours after training (20 min), and over the weekend (36 h). Experiments were conducted during the light phase of the light–dark cycle (between 0900 and 1200 h) and were carried out in accordance with the National Institutes of Health Guide for the Care and Use of Laboratory Animals (2011) and with the approval of the Institutional Animal Care and Use Committee at University of Texas Medical Branch.

**Drug Discrimination Procedures.** Full experimental details of the procedures and analyses have been previously described.<sup>23, 34, 41, 49</sup> Briefly, standard two-lever, water-reinforced drug discrimination procedures were used (Med Associates, St. Albans, USA). Each chamber was equipped with a water-filled dispenser mounted equidistantly between two retractable response levers on the wall and housed in a light- and sound-proof cubicle. Illumination came from a 28V house light; ventilation and masking noise were provided by a ventilation fan. A computer with Med-PC IV software was used to run programs and record all experimental events.

Rats were trained to discriminate an injection of WAY163909 (0.75 mg/kg; 1.0 mL/kg, ip) from saline (1.0 mL/kg, ip) administered 15 min before start of training sessions. Daily sessions lasted 15 min and were conducted Monday through Friday. During the phase of errorless training, only the stimulus-appropriate (drug or saline) lever was present. Training began under a fixed ratio 1 (FR1) schedule of water reinforcement, and the FR requirement was incremented until all animals

1  
2  
3 were responding reliably under an FR20 schedule for each experimental condition. Left and right  
4  
5 levers were counterbalanced across rats for WAY163909/saline assignments. During this phase of  
6  
7 training, WAY163909 and saline were administered randomly with the restriction that neither  
8  
9 condition prevailed for more than three consecutive sessions. After responding stabilized, both  
10  
11 levers were introduced simultaneously during 15 min training sessions. The rats were required to  
12  
13 respond on the stimulus-appropriate (correct) lever to obtain water reinforcement. There were no  
14  
15 programmed consequences for responding on the incorrect lever. This phase of training continued  
16  
17 until the performance of all rats attained criterion (defined as mean accuracies of at least 80%  
18  
19 stimulus-appropriate responding for ten consecutive sessions).  
20  
21  
22

23  
24 Test sessions were initiated and conducted once or twice per week; with training sessions  
25  
26 completed on intervening days. Rats were required to maintain accuracies >80% correct for saline  
27  
28 and WAY163909 maintenance sessions, which immediately preceded all tests. During test  
29  
30 sessions, animals were placed in the chambers and, upon completion of 20 responses on either  
31  
32 lever, a single water reinforcer was delivered, and the house lights were turned off. The rat was  
33  
34 removed from the chamber and returned to the colony. The test sessions were terminated after 15  
35  
36 min if the rats did not complete 20 responses on either lever; only data from rats that completed  
37  
38 the test were included in data analysis. In substitution tests, rats were administered compound **12**  
39  
40 (0.5, 1.0, 2.0, 5.0 mg/kg, ip) 30 min before the start of the test. WAY163909 (0.125, 0.25, 0.5,  
41  
42 0.625, 0.75, or 1.0 mg/kg, ip), or saline was administered 15 min prior to the start of the test. In  
43  
44 combination tests, rats were tested for lever selection following administration of compound **12**  
45  
46 (0, 0.5, 1.0, or 2.0 mg/kg, ip) or vehicle 30 min and WAY163909 (0.5 mg/kg ip) or saline 15 min  
47  
48 before start of the test. In combination tests, SB242084 (0.5 mg/kg) was administered 15 min  
49  
50 before administration of WAY163909. The dose of WAY163909 (0.5 mg/kg, ip) employed evoked  
51  
52  
53  
54  
55  
56  
57  
58  
59  
60

~50% drug-appropriate responding. Full substitution was defined as  $\geq 80\%$  of rats selecting the WAY163909-appropriate lever. Partial substitution was defined as  $\geq 40\%$  and  $< 80\%$  drug-appropriate responding.

**Statistical Analyses.** All treatment assignments were blinded to investigators who performed *in vivo* assays and endpoint statistical analyses. Rat performance in training and test sessions was expressed as the average percentage of rats selecting the WAY163909-associated lever because responding is typically a quantal rather than continuous function of stimulus similarity in the two-choice drug discrimination assay.<sup>23, 34-42</sup> Thus, intermediate doses of the training drug or substitution test responses are typically confined to one lever. During test sessions, the lever selection is defined by the initial FR20 schedule completion at which point the test terminates and the animal is removed from the chamber without delivery of a reinforcer. Logistic regression analyses were used to determine the effects of increasing doses of WAY163909, compound **12**, or combination treatments on the probability that rats responded on the WAY163909-associated lever (binary response variable). The response rate (responses per minute) was calculated as the total number of responses emitted before completion of the first FR 20 divided by the number of minutes taken to complete the first ratio. Response rates were analyzed using one-way ANOVA with Dunnett's correction for comparisons to vehicle or control groups. Log-probit analyses were used to estimate the dose of WAY163909 predicted to elicit 50% WAY163909-associated lever responses (ED<sub>50</sub>). All statistical significance was set at an experimenter-wise error rate of  $\alpha = 0.05$ .

## AUTHOR INFORMATION

### Corresponding Author

Jia Zhou, Ph.D.: Tel: (409) 772-9748; Fax: (409) 772-9648; E-mail: jizhou@utmb.edu.

Kathryn A. Cunningham, Ph.D.: Tel: (409)-772-9629; Fax: (409)-772-7050; E-mail: kcunning@utmb.edu.

Noelle C. Anastasio, Ph.D.: Tel: (409)-772-9656; Fax: (409)-772-7050; E-mail: ncanasta@utmb.edu.

### Author Contributions

J.Z., K.A.C., and N.C.A. developed the concepts and approaches as well as supervised the work. E.A.W, C.T.W., and J.C. synthesized, purified, and characterized the reported compounds. E.A.W. performed the molecular docking and computational modeling. E.J.G., N.C.A., K.A.C, J.M.M., C.A.S, and K.P. performed and/or analyzed the *in vitro* cellular studies. E.J.G., R.G.F., K.A.C., and N.C.A. performed and/or analyzed the *in vivo* studies. E.A.W., E.J.G., K.A.C., N.C.A. and J.Z., wrote the manuscript.

### ACKNOWLEDGMENTS

This work was supported by grants R21 MH093844 (JZ/KAC), R01 DA038446 (JZ/KAC), K05 DA020087 (KAC), P30 DA28821 (KAC), T32 DA07287 (CTW and EAW), F31 DA038922 (CTW), and F31 DA045511 (EAW) from the National Institutes of Health, the John D. Stobo, M.D. Distinguished Chair Endowment Fund (J.Z.), the Center for Addiction Research at UTMB, R.A. Welch Foundation Chemistry and Biology Collaborative Grant from Gulf Coast Consortia (GCC) for Chemical Genomics, a training fellowship from the Keck Center for Interdisciplinary

Bioscience Training of the GCC (NIGMS grant T32 GM089657-03 (CTW), Sealy and Smith Foundation grant (to the Sealy Center for Structural Biology and Molecular Biophysics), and the John Sealy Memorial Endowment Fund. We thank Drs. Lawrence C. Sowers, Jason Herring, and Tianzhi Wang for the NMR spectroscopy assistance; Sonja J. Stutz assisted in some *in vivo* studies; Claudia M. Crawford, Carrie E. McAllister and Konrad Pazdrak for conducting *in vitro* assays; and Marcy B. Jordan for helpful discussions during the development of this project. Receptor binding profiles and agonist functional data was generously provided by the National Institute of Mental Health Psychoactive Drug Screening Program (PDSP), Contract #HHSN-271-2013-00017-C (NIMH PDSP). The NIMH PDSP is directed by Dr. Bryan L. Roth at the University of North Carolina at Chapel Hill and Project Officer Jamie Driscoll at NIMH, Bethesda MD, USA.

## ABBREVIATIONS USED

Serotonin, 5-HT; 5-HT<sub>2A</sub> receptor, 5-HT<sub>2AR</sub>; 5-HT<sub>2B</sub> receptor, 5-HT<sub>2BR</sub>; 5-HT<sub>2C</sub> receptor, 5-HT<sub>2CR</sub>; Central nervous system, CNS; G protein-coupled receptor, GPCR; Substance Use Disorder, SUD; U.S. Food and Drug Administration, FDA; Body Mass Index, BMI; positive allosteric modulator, PAM; negative allosteric modulator, NAM; lipophilic tail, LT; polar head, PH; structure-activity relationship, SAR; *N,N,N',N'*-tetramethyl-*O*-(1*H*-benzotriazol-1-yl)uronium hexafluorophosphate, HBTU; *N,N*-diisopropylethylamine, DIPEA; trifluoroacetic acid, TFA; preparative thin layer chromatographic, PTLC; phospholipase C $\beta$ , PLC $\beta$ ; inositol-1,4,5-trisphosphate, IP<sub>3</sub>; diacylglycerol, DAG; Intracellular calcium, Ca<sub>i</sub><sup>2+</sup>; Chinese hamster ovary, CHO; 2-hydroxypropyl- $\beta$ -cyclodextrin, HP- $\beta$ -CD; half-life, *t*<sub>1/2</sub>; time of maximum concentration, T<sub>max</sub>; plasma clearance, CL; volume of distribution, V<sub>ss</sub>; maximum concentration,



$C_{\max}$ ; area under the plasma concentration–time curve,  $AUC_{0-\infty}$ ; oral bioavailability,  $F$ ; intraperitoneal, IP; intravenous, IV; Madin-Darby Canine Kidney, MDCK; multiparameter optimization (MPO); P-glycoprotein, P-gp; phospholipase D, PLD; pharmacokinetics, PK; extracellular loop, ECL; transmembrane helix, TM; Support vector machine, SVM.

## ASSOCIATED CONTENT

### Supporting Information

Calculated physicochemical properties, radioligand binding data, cytotoxicity data, additional cellular assay data, docking protocol,  $^1\text{H}$  and  $^{13}\text{C}$  NMR spectra for the compounds described in this paper, and Molecular Formula Strings. This material is available free of charge via the Internet at <http://pubs.acs.org>.

### Conflicts of Interest

The authors declare no competing financial interests.

## REFERENCES

1. Zhou, J.; Cunningham, K. A. Positive Allosteric Modulation of the 5-HT<sub>2C</sub> Receptor: Implications for Neuropsychopharmacology and Neurotherapeutics. *Neuropsychopharmacology* **2019**, 44, 230-231.

2. Tecott, L. H.; Sun, L. M.; Akana, S. F.; Strack, A. M.; Lowenstein, D. H.; Dallman, M. F.; Julius, D. Eating Disorder and Epilepsy in Mice Lacking 5-HT<sub>2c</sub> Serotonin Receptors. *Nature* **1995**, 374, 542-546.
3. Ge, T.; Zhang, Z.; Lv, J.; Song, Y.; Fan, J.; Liu, W.; Wang, X.; Hall, F. S.; Li, B.; Cui, R. The Role of 5-HT<sub>2c</sub> Receptor on Corticosterone-mediated Food Intake. *J. Biochem. Mol. Toxicol.* **2017**, 31, DOI: 10.1002/jbt.21890.
4. Halford, J. C.; Lawton, C. L.; Blundell, J. E. The 5-HT<sub>2</sub> Receptor Agonist MK-212 Reduces Food Intake and Increases Resting but Prevents the Behavioural Satiety Sequence. *Pharmacol. Biochem. Behav.* **1997**, 56, 41-46.
5. Wacker, D. A.; Miller, K. J. Agonists of the Serotonin 5-HT<sub>2C</sub> Receptor: Preclinical and Clinical Progression in Multiple Diseases. *Curr. Opin. Drug Discov. Devel.* **2008**, 11, 438-445.
6. Dunlop, J.; Sabb, A. L.; Mazandarani, H.; Zhang, J.; Kalgaonker, S.; Shukhina, E.; Sukoff, S.; Vogel, R. L.; Stack, G.; Schechter, L.; Harrison, B. L.; Rosenzweig-Lipson, S. WAY-163909 [(7bR, 10aR)-1,2,3,4,8,9,10,10a-Octahydro-7bH-cyclopenta-[b][1,4]diazepino[6,7,1hi]indole], a Novel 5-Hydroxytryptamine 2C Receptor-selective Agonist with Anorectic Activity. *J. Pharmacol. Exp. Ther.* **2005**, 313, 862-869.
7. Howell, L. L.; Cunningham, K. A. Serotonin 5-HT<sub>2</sub> Receptor Interactions with Dopamine Function: Implications for Therapeutics in Cocaine Use Disorder. *Pharmacol. Rev.* **2015**, 67, 176-197.
8. Bubar, M. J.; Cunningham, K. A. Prospects for Serotonin 5-HT<sub>2R</sub> Pharmacotherapy in Psychostimulant Abuse. *Prog. Brain Res.* **2008**, 172, 319-346.
9. Anastasio, N. C.; Stutz, S. J.; Fox, R. G.; Sears, R. M.; Emeson, R. B.; DiLeone, R. J.; O'Neil, R. T.; Fink, L. H.; Li, D.; Green, T. A.; Moeller, F. G.; Cunningham, K. A. Functional

Status of the Serotonin 5-HT<sub>2C</sub> Receptor (5-HT<sub>2CR</sub>) Drives Interlocked Phenotypes that Precipitate Relapse-like Behaviors in Cocaine Dependence. *Neuropsychopharmacology* **2014**, 39, 370-382.

10. Neelakantan, H.; Holliday, E. D.; Fox, R. G.; Stutz, S. J.; Comer, S. D.; Haney, M.; Anastasio, N. C.; Moeller, F. G.; Cunningham, K. A. Lorcaserin Suppresses Oxycodone Self-administration and Relapse Vulnerability in Rats. *ACS Chem. Neurosci.* **2017**, 8, 1065-1073.

11. Moeller, F. G.; Cunningham, K. A. Innovative Therapeutic Intervention for Opioid Use Disorder. *Neuropsychopharmacology* **2018**, 43, 220-221.

12. Shanahan, W. R.; Rose, J. E.; Glicklich, A.; Stubbe, S.; Sanchez-Kam, M. Lorcaserin for Smoking Cessation and Associated Weight Gain: a Randomized 12-week Clinical Trial. *Nicotine Tob. Res.* **2017**, 19, 944-951.

13. Farr, O. M.; Upadhyay, J.; Gavrieli, A.; Camp, M.; Spyrou, N.; Kaye, H.; Mathew, H.; Vamvini, M.; Koniaris, A.; Kilim, H.; Srnka, A.; Migdal, A.; Mantzoros, C. S. Lorcaserin Administration Decreases Activation of Brain Centers in Response to Food Cues and These Emotion- and Salience-related Changes Correlate with Weight Loss Effects: a 4-Week-long Randomized, Placebo-controlled, Double-blind Clinical Trial. *Diabetes* **2016**, 65, 2943-2953.

14. Anastasio, N. C.; Liu, S.; Maili, L.; Swinford, S. E.; Lane, S. D.; Fox, R. G.; Hamon, S. C.; Nielsen, D. A.; Cunningham, K. A.; Moeller, F. G. Variation Within the Serotonin (5-HT) 5-HT<sub>2C</sub> Receptor System Aligns with Vulnerability to Cocaine Cue Reactivity. *Transl. Psychiatry* **2014**, 4, e369.

15. Everitt, B. J.; Robbins, T. W. Drug Addiction: Updating Actions to Habits to Compulsions Ten Years On. *Annu. Rev. Psychol.* **2016**, 67, 23-50.

16. Nichols, D. E. Hallucinogens. *Pharmacol. Ther.* **2004**, 101, 131-181.

17. Fitzgerald, L. W.; Burn, T. C.; Brown, B. S.; Patterson, J. P.; Corjay, M. H.; Valentine, P. A.; Sun, J. H.; Link, J. R.; Abbaszade, I.; Hollis, J. M.; Largent, B. L.; Hartig, P. R.; Hollis, G. F.; Meunier, P. C.; Robichaud, A. J.; Robertson, D. W. Possible Role of Valvular Serotonin 5-HT<sub>2B</sub> Receptors in the Cardiopathy Associated with Fenfluramine. *Mol. Pharmacol.* **2000**, *57*, 75-81.
18. Wild, C.; Cunningham, K. A.; Zhou, J. Allosteric Modulation of G Protein-Coupled Receptors: An Emerging Approach of Drug Discovery. *Austin J. Pharmacol. Ther.* **2014**, *2*, 1-8.
19. Wold, E. A.; Zhou, J. GPCR Allosteric Modulators: Mechanistic Advantages and Therapeutic Applications. *Curr. Top. Med. Chem.* **2018**, *18*, 2002-2006.
20. Wold, E. A.; Chen, J.; Cunningham, K. A.; Zhou, J. Allosteric Modulation of Class A GPCRs: Targets, Agents, and Emerging Concepts. *J. Med. Chem.* **2019**, *62*, 88-127.
21. Im, W. B.; Chio, C. L.; Alberts, G. L.; Dinh, D. M. Positive Allosteric Modulator of the Human 5-HT<sub>2C</sub> Receptor. *Mol. Pharmacol.* **2003**, *64*, 78-84.
22. Ding, C.; Bremer, N. M.; Smith, T. D.; Seitz, P. K.; Anastasio, N. C.; Cunningham, K. A.; Zhou, J. Exploration of Synthetic Approaches and Pharmacological Evaluation of PNU-69176E and its Stereoisomer as 5-HT<sub>2C</sub> Receptor Allosteric Modulators. *ACS Chem. Neurosci.* **2012**, *3*, 538-545.
23. Wild, C. T.; Miszkiel, J. M.; Wold, E. A.; Soto, C. A.; Ding, C.; Hartley, R. M.; White, M. A.; Anastasio, N. C.; Cunningham, K. A.; Zhou, J. Design, Synthesis, and Characterization of 4-Undecylpiperidine-2-carboxamides as Positive Allosteric Modulators of the Serotonin (5-HT) 5-HT<sub>2C</sub> Receptor. *J. Med. Chem.* **2019**, *62*, 288-305.
24. Garcia-Carceles, J.; Decara, J. M.; Vazquez-Villa, H.; Rodriguez, R.; Codesido, E.; Cruces, J.; Brea, J.; Loza, M. I.; Alen, F.; Botta, J.; McCormick, P. J.; Ballesteros, J. A.; Benhamu, B.;

Rodriguez de Fonseca, F.; Lopez-Rodriguez, M. L. A Positive Allosteric Modulator of the Serotonin 5-HT<sub>2C</sub> Receptor for Obesity. *J. Med. Chem.* **2017**, *60*, 9575-9584.

25. Singh, K.; Sona, C.; Ojha, V.; Singh, M.; Mishra, A.; Kumar, A.; Siddiqi, M. I.; Tripathi, R. P.; Yadav, P. N. Identification of Dual Role of Piperazine-linked Phenyl Cyclopropyl Methanone as Positive Allosteric Modulator of 5-HT<sub>2C</sub> and Negative Allosteric Modulator of 5-HT<sub>2B</sub> Receptors. *Eur. J. Med. Chem.* **2019**, *164*, 499-516.

26. Seitz, P. K.; Bremer, N. M.; McGinnis, A. G.; Cunningham, K. A.; Watson, C. S. Quantitative Changes in Intracellular Calcium and Extracellular-regulated Kinase Activation Measured in Parallel in CHO Cells Stably Expressing Serotonin (5-HT) 5-HT<sub>2A</sub> or 5-HT<sub>2C</sub> Receptors. *BMC Neurosci.* **2012**, *13*, 25.

27. Wold, E. A.; Wild, C. T.; Cunningham, K. A.; Zhou, J. Targeting the 5-HT<sub>2C</sub> Receptor in Biological Context and the Current State of 5-HT<sub>2C</sub> Receptor Ligand Development. *Curr. Top. Med. Chem.* **2019**, *19*, 1381-1398.

28. Peng, Y.; McCorvy, J. D.; Harpsoe, K.; Lansu, K.; Yuan, S.; Popov, P.; Qu, L.; Pu, M.; Che, T.; Nikolajsen, L. F.; Huang, X. P.; Wu, Y.; Shen, L.; Bjorn-Yoshimoto, W. E.; Ding, K.; Wacker, D.; Han, G. W.; Cheng, J.; Katritch, V.; Jensen, A. A.; Hanson, M. A.; Zhao, S.; Gloriam, D. E.; Roth, B. L.; Stevens, R. C.; Liu, Z. J. 5-HT<sub>2C</sub> Receptor Structures Reveal the Structural Basis of GPCR Polypharmacology. *Cell* **2018**, *172*, 719-730 e714.

29. Manivet, P.; Schneider, B.; Smith, J. C.; Choi, D. S.; Maroteaux, L.; Kellermann, O.; Launay, J. M. The Serotonin Binding Site of Human and Murine 5-HT<sub>2B</sub> Receptors: Molecular Modeling and Site-Directed Mutagenesis. *J. Biol. Chem.* **2002**, *277*, 17170-17178.

30. Song, K.; Liu, X.; Huang, W.; Lu, S.; Shen, Q.; Zhang, L.; Zhang, J. Improved Method for the Identification and Validation of Allosteric Sites. *J. Chem. Inf. Model.* **2017**, *57*, 2358-2363.

- 1  
2  
3 31. Banerjee, P.; Eckert, A. O.; Schrey, A. K.; Preissner, R. ProTox-II: A Webserver for the  
4 Prediction of Toxicity of Chemicals. *Nucleic Acids Res.* **2018**, 46, W257-W263.  
5  
6  
7 32. Wager, T. T.; Hou, X.; Verhoest, P. R.; Villalobos, A. Moving Beyond Rules: The  
8 Development of a Central Nervous System Multiparameter Optimization (CNS MPO) Approach  
9 to Enable Alignment of Druglike Properties. *ACS Chem. Neurosci.* **2010**, 1, 435-449.  
10  
11  
12 33. Shaffer, C. L. Defining Neuropharmacokinetic Parameters in CNS Drug Discovery to  
13 Determine Cross-Species Pharmacologic Exposure–Response Relationships. In *Annual Reports in*  
14 *Medicinal Chemistry*, Macor, J. E., Ed. Academic Press: 2010; Vol. 45, pp 55-70.  
15  
16  
17 34. Soto, C. A.; Du, H. C.; Fox, R. G.; Yang, T.; Hooson, J.; Anastasio, N. C.; Gilbertson, S.  
18 R.; Cunningham, K. A. In Vivo and In Vitro Analyses of Novel Peptidomimetic Disruptors for the  
19 Serotonin 5-HT<sub>2C</sub> Receptor Interaction With Phosphatase and Tensin Homolog. *Front.*  
20 *Pharmacol.* **2019**, 10, 907.  
21  
22  
23 35. Colpaert, F. C. Drug Discrimination in Neurobiology. *Pharmacol. Biochem. Behav.* **1999**,  
24 64, 337-345.  
25  
26  
27 36. Colpaert, F. C. Drug Discrimination: Methods of Manipulation, Measurement, and  
28 Analysis. In *Methods of Assessing the Reinforcing Properties of Abused Drugs*, Bozarth, M. A.,  
29 Ed. Springer New York: New York, NY, 1987; pp 341-372.  
30  
31  
32 37. Colpaert, F. C.; Janssen, P. A. Agonist and Antagonist Effects of Prototype Opiate Drugs  
33 in Rats Discriminating Fentanyl from Saline: Characteristics of Partial Generalization. *J.*  
34 *Pharmacol. Exp. Ther.* **1984**, 230, 193-199.  
35  
36  
37 38. Negus, S. S.; Banks, M. L. Pharmacokinetic-Pharmacodynamic (PKPD) Analysis with  
38 Drug Discrimination. *Curr. Top. Behav. Neurosci.* **2018**, 39, 245-259.  
39  
40  
41  
42  
43  
44  
45  
46  
47  
48  
49  
50  
51  
52  
53  
54  
55  
56  
57  
58  
59  
60

39. McCreary, A. C.; Filip, M.; Cunningham, K. A. Discriminative Stimulus Properties of (+/-)-Fenfluramine: the Role of 5-HT<sub>2</sub> Receptor Subtypes. *Behav. Neurosci.* **2003**, 117, 212-221.
40. Callahan, P. M.; Cunningham, K. A. Involvement of 5-HT<sub>2C</sub> Receptors in Mediating the Discriminative Stimulus Properties of m-Chlorophenylpiperazine (mCPP). *Eur. J. Pharmacol.* **1994**, 257, 27-38.
41. Frankel, P. S.; Cunningham, K. A. m-Chlorophenylpiperazine (mCPP) Modulates the Discriminative Stimulus Effects of Cocaine Through Actions at the 5-HT<sub>2C</sub> Receptor. *Behav. Neurosci.* **2004**, 118, 157-162.
42. Glennon, R. A.; Young, R. Drug Discrimination and Development of Novel Agents and Pharmacological Tools. In *Drug Discrimination: Applications to Medicinal Chemistry and Drug Discovery*, Glennon, R. A.; Young, R., Eds. John Wiley and Sons: Hoboken, NJ: 2011; pp 217-238.
43. Mathis, D. A.; Emmett-Oglesby, M. W. Quantal vs. Graded Generalization in Drug Discrimination: Measuring a Graded Response. *J. Neurosci. Methods.* **1990**, 31, 23-33.
44. Kennett, G. A.; Wood, M. D.; Bright, F.; Trail, B.; Riley, G.; Holland, V.; Avenell, K. Y.; Stean, T.; Upton, N.; Bromidge, S.; Forbes, I. T.; Brown, A. M.; Middlemiss, D. N.; Blackburn, T. P. SB 242084, a Selective and Brain Penetrant 5-HT<sub>2C</sub> Receptor Antagonist. *Neuropharmacology* **1997**, 36, 609-620.
45. Fronik, P.; Gaiser, B. I.; Sejer Pedersen, D. Bitopic Ligands and Metastable Binding Sites: Opportunities for G Protein-Coupled Receptor (GPCR) Medicinal Chemistry. *J. Med. Chem.* **2017**, 60, 4126-4134.
46. Gaiser, B. I.; Danielsen, M.; Marcher-Rørsted, E.; Røpke Jørgensen, K.; Wróbel, T. M.; Frykman, M.; Johansson, H.; Bräuner-Osborne, H.; Gloriam, D. E.; Mathiesen, J. M.; Sejer

Pedersen, D. Probing the Existence of a Metastable Binding Site at the  $\beta$ 2-Adrenergic Receptor with Homobivalent Bitopic Ligands. *J. Med. Chem.* **2019**, 62, 7806-7839.

47. Dror, R. O.; Pan, A. C.; Arlow, D. H.; Borhani, D. W.; Maragakis, P.; Shan, Y.; Xu, H.; Shaw, D. E. Pathway and Mechanism of Drug Binding to G-Protein-Coupled Receptors. *Proc. Nat. Acad. Sci.* **2011**, 108, 13118.

48. Zhou, J.; Ding, C.; Cunningham, K. A. Allosteric Modulators of 5-Hydroxytryptamine 2C Receptor (5-HT<sub>2</sub>CR). US9533973B2, 2017.

49. Filip, M.; Bubar, M. J.; Cunningham, K. A. Contribution of Serotonin (5-HT) 5-HT<sub>2</sub> Receptor Subtypes to the Discriminative Stimulus Effects of Cocaine in Rats. *Psychopharmacology* **2006**, 183, 482-489.



## Table of Contents (TOC) Graphic

